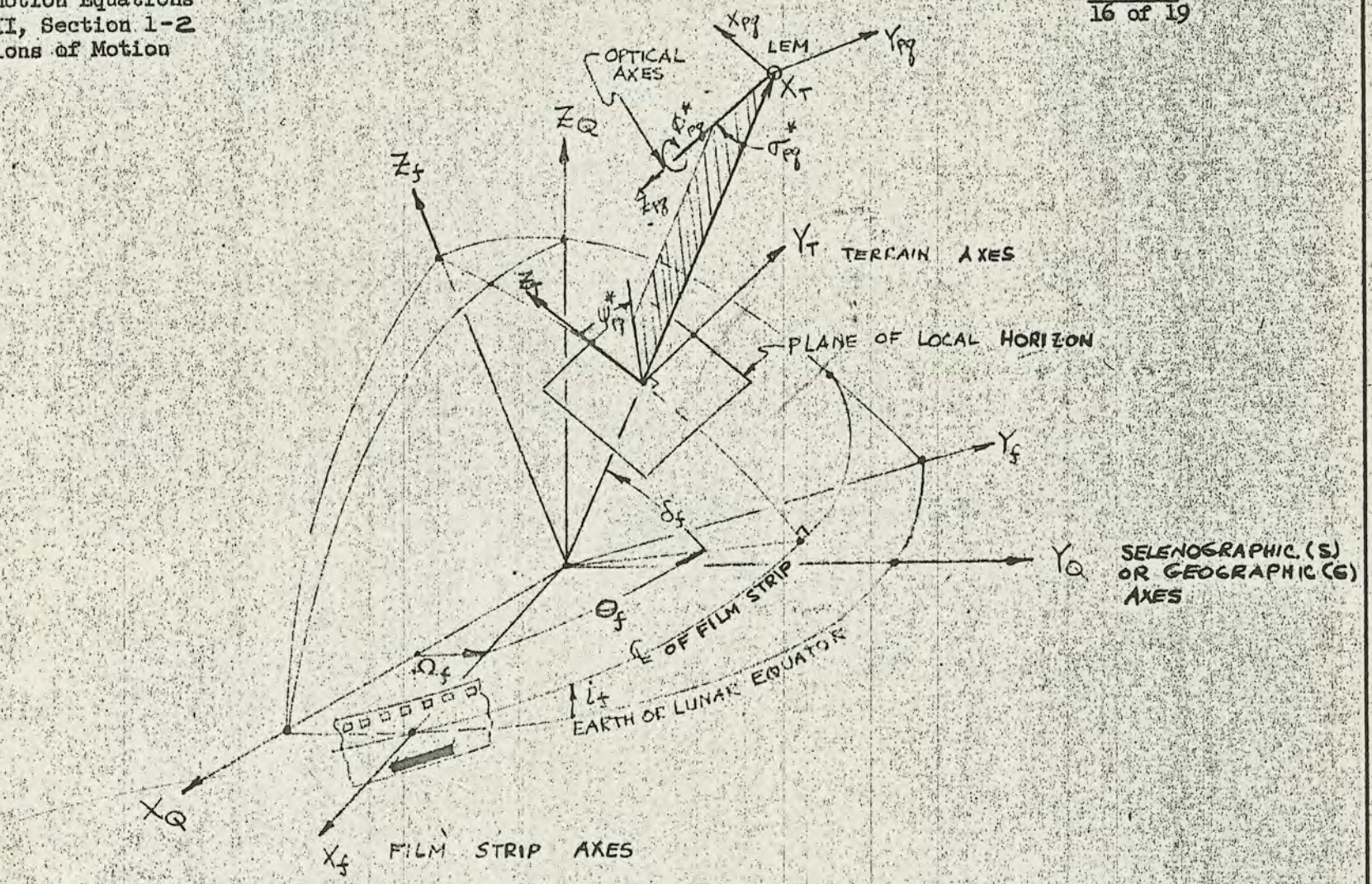

FIGURE-16. MISSON EFFECTS PROJECTOR

Figure 17. Not used

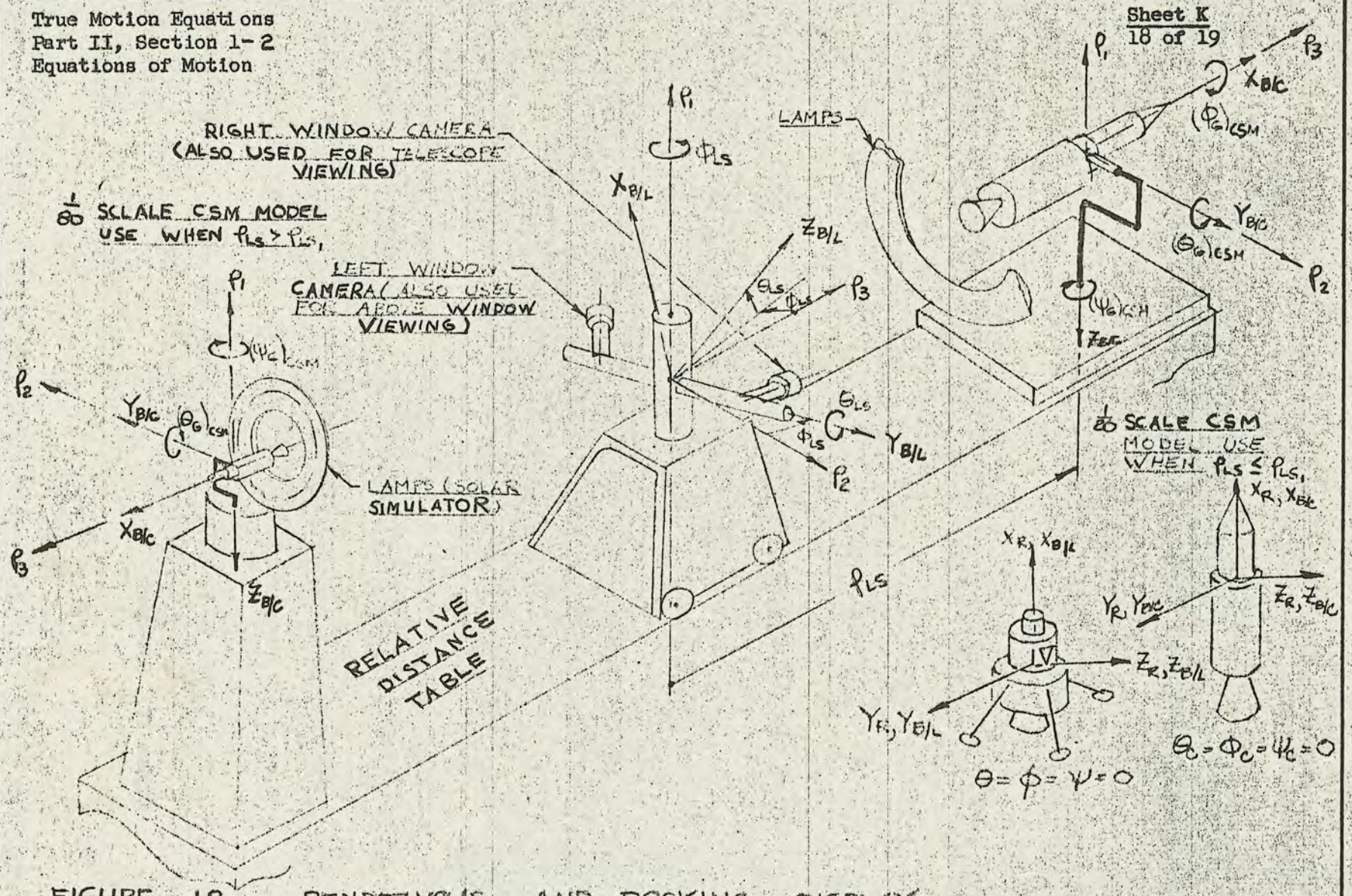

FIGURE - 18. RENDEZVOUS AND DOCKING DISPLAY

FORM G328 5-63 (ENG 23, ENG 26)
GRUMMAN AIRCRAFT ENGINEERING CORPORATION
16-93
REPORT LED-440-3
DATE 8/65
CODE 26512

True Motion Equations
Part II, Section 1-2
Equations of Motion

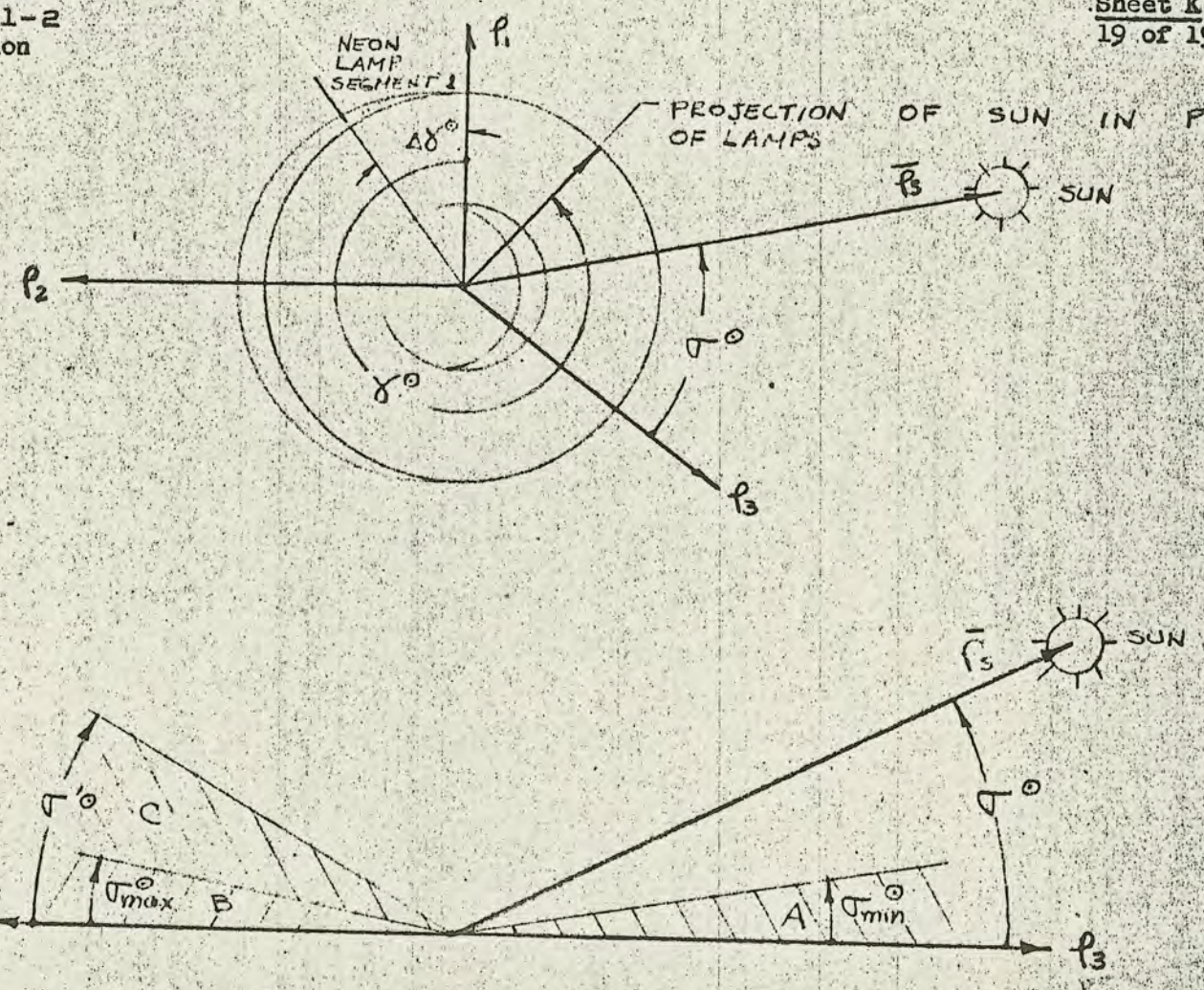

FIGURE-19. CSM-SUN ILLUMINATION DISPLAY

TRUE MOTION EQUATIONS

Part II LMS Data

Section 1. Equations of Motion

3. Equation Documentation

3. Equation Documentation

Table of Contents

1126

5. Matrix Operator From Inertial E - Frame to Geographic G - Frame
6. Matrix Operator From the LEM Body B - Frame to the Optical Window W - Frame Or Telescope T - Frame

E. Ephemeris
1. Purpose
2. Problem Start Initialization
3. Lunar - Solar Positional and Orbital Elements

F. Rendezvous Radar
1. Purpose
2. Relative Range and Velocity Vectors Measured in LEM Body Axes
3. Rendezvous Radar Interface Parameters

G. Landing Radar
1. Purpose
2. Doppler Input Velocities
3. Slant Range Measured Along Radar Beams
4. Land Mass Simulator

H. LEM Communication Requirements
1. Purpose
2. LEM - CSM Communication Capability
3. LEM - Earth Tracking Station Communication Capability

I. Weights and Balance Calculations
1. Purpose
2. LEM Mass
3. Instantaneous Center-of-Gravity
4. Moments and Products of Inertia

J. Visual Displays
1. Purpose
2. Lunar and Solar Occulters
3. Mission Effects Projector
4. Landing and Ascent Image Generator
5. Rendezvous and Docking Simulator

IV. References

I. Summary

The purpose of this section is to present the rationale, assumptions and derivations used to generate the Category 1 detailed equations appearing in Section 1-2. Category 1 equations provide "true" (error free) trajectory information to all major subsystems and the instructor, in addition to generating true visual cues for the astronaut.

Refer to Section 2 for Category 2 equations. Category 2 will describe all Primary Guidance and Navigation System (PGNS) equations (Sheets L through Q) together with IMU and AOT full subsystem equations. Category 2 equations provide indicated rather than true trajectory information, and control input data for the Stabilization and Main Engine Math Models.

II. Introduction

The LMS Math Model has been written in accordance with the ground rules established in reference 1. These are:

1. The LMS must operate either independently of the AMS and MCC-H or in conjunction with the AMS and/or MCC-H (integrated mode).

2. The LMS must be capable of simulating either Lunar Mission or Earch Mission phases.

3. The LMS must describe all LEM operational functions.

Format. - Category 1 information contained herein is outlined in accordance with the Level I Index Diagram given in Sheet AAA. Sheet AAA contains 10 sets of equations, 1 set of figures, and a Math Model Interface Listing. Each set is lettered from A to K. Furthermore, each set is partitioned into subsets numbered from 10 to 90. Thus, block F-20 describes the rendezvous radar gimbal angle and gimbal angle rate equations shown on sheet F block 20.

Sheet AAA also presents representative inputs from other math models. External math model inputs are indicated by arrows entering from the left of each set. The more important category 1 outputs, computed within each set, are shown by arrows leaving the set.

A more detailed breakdown of the flow between sets, subsets, and other math models are shown in sheets AA - Level II Flow Diagrams. Level II Diagrams were generated as an aid to programming the equations on a digital computer.

Paragraph III describes the detailed equations developed on Sheets A through J (Level III Detailed Flow Diagrams). Subsections are lettered to correspond to those sets shown in index Sheet AAA. For example, subsection III-J discusses the External Visual Display Equipment drive equations. Each subsection is complete and includes:

a. The purpose or reasons for simulating each set

b. Derivations and assumptions related to the subset equations

Equations designated by a capital letter followed by a number can be found on the corresponding Level III Flow Diagrams. Equations designated by small letters are used as intermediaries to derive a set or subset equation, or to present an alternate approach not listed on the Level III flow diagram.

Symbols, units and range of variables are defined in Section 1-1. References are listed in paragraph IV. Levels I, II, and III Flow Diagrams are located in Section 1-2.

Figure numbers appearing in Section 1-3-III refer to the figure numbers of Sheet K located in Section 1-2.

III. Category 1 Equations (Equations of Motion) - Sheets A through J

A. LEM Translational Equations (M Frame)

1. Purpose. - The purpose of Set "A" equations is to accurately represent all significant external forces acting on the LEM vehicle during the lunar mission phase. Integrating these forces provides a "true" LEM trajectory governed by the accuracy of the physical assumptions and the numerical integration scheme employed. These equations will be used during independent or integrated lunar operational modes only. Earth operational modes and CSM motion equations during the independent mode are discussed in paragraph III-B.

1130

2. Primary Reference System and Generalized Equations of Motion. - Reference 2 indicates that the primary reference frame will be defined by the mean Earth equator of date, where, axis X is directed along the mean equinox of date and axis Z lies along the Earth's mean spin vector. During lunar missions, the reference set will be Moon centered (X_M, Y_M, Z_M; see Sheet K, Figure 1) whereas, during Earth training missions the reference set will be earth centered (X_E, Y_E, Z_E).

The equations of motion of a point mass relative to an inertial frame centered at a massive body, n, are as follows:

$$\ddot{\bar{r}}_L = -k^2(m_n+m_L)\frac{\bar{r}_L}{r_L^3} - k^2\sum_j m_j\left[\frac{\bar{r}_L-\bar{r}_J}{r_{JL}^3} + \frac{\bar{r}_J}{r_J^3}\right] + \bar{P} + \sum\frac{\bar{F}}{m_L} \qquad (a-1)$$

Subscript L denotes LEM. Let the massive body represent the moon, n = M. The bracketed term contains both the direct attraction of body m_j on the vehicle m_L and the indirect attraction of body m_j on the moon's origin m_m. Vector $\bar{P}$ denotes the lunar triaxiality acceleration. All external forces such as main engine thrust, RCS thrust, fuel slosh, separation forces and jet damping forces are lumped into the term $\sum\frac{\bar{F}}{m_L}$.

In order to inhibit the normal equations of motion, when the vehicle has landed on the lunar surface, the following steps are taken:

1. When the boolean term B_{1151} indicating touchdown is received by the equations of motion, the integrations yielding $\dot{r}_{M/L}$ are inhibited and $\dot{r}_{M/L}$ is set equal to the velocity of the Moon with respect to the M-Frame ($\dot{r}_{M/L}$ from G-10).

   In this way the position of the LEM in the M-frame is integrated as usual with velocities proportional to the lunar rotation.

1131

2. In order for the vehicle to "break ground" on ascent, a test is made to determine the radial acceleration of the vehicle

$$\ddot{r}_{M/L} = \frac{\ddot{X}_{M/L} X_{ML} + \ddot{Y}_{M/L} Y_{M/L} + \ddot{Z}_{M/L} Z_{M/L}}{r_{M/L}} \quad (A-14)$$

if this value is greater than the gravitational acceleration:

$$\ddot{r}_{M/L} \geq \frac{\mu_M}{r_{M/L}} \quad (A-14)$$

a boolean B_1 is generated which allows the normal equations of motion to again operate

$$\dot{r}_{M/L} = (\bar{B}_{1151} + B_1) \int \ddot{r}_{M/L}\, dt + B_{1151}\, \dot{r}_{M/S} \quad (A-11)$$

3. Gravitational Perturbations. - During the lunar mission phase all gravitational forces except those due to lunar triaxiality are neglected. The reasons for this statement are listed below.

a. "M or E" - Frame Perturbation. - Lunar-solar forces acting on the Earth's equatorial bulge cause the Earth's mean equator of date, and hence the mean equinox, to precess at an average rate of about 0.015 degrees/year. Accordingly, the reference M frame is non-inertial. An inertial set, however, is assumed. Solution accuracy is not compromised by this assumption because it can be shown that the apparent coriolis and centrifugal errors induced are less than those perturbative accelerations due to either Mars or Jupiter (reference 3). On a short term basis, the LEM trajectory is therefore unaffected.

b. Solar Perturbation. - An extensive numerical study has been conducted at GAEC (reference 4) to ascertain the effect of lunar triaxiality, Earth, Sun and planet perturbations on the motion of a close lunar satellite. This report clearly indicates that the effect of solar and planetary (earth excluded) perturbations on satellite motion are approximately 3 to 4 orders of magnitude smaller than the combined Earth-lunar triaxiality perturbations. This is in general agreement with the expected order of magnitude obtained by taking the ratio between the sun and triaxiality perturbations. Since the Earth perturbation is neglected, it is safe to neglect the solar and planetary perturbations for LEM simulation.

c. Earth Perturbation. - The influence of the Earth's perturbative acceleration on the motion of a near lunar satellite has a smaller effect than does the moon's triaxiality perturbation. This is evidenced either from inspecting the Earth-Moon potential function or by comparing the data given in reference 4. Numerical data from reference 4 indicate that the Earth perturbation has approximately a 1 to 2 order of magnitude smaller effect on short period radial, semi-major axis, and eccentricity excursions (for a low altitude, circular, equatorial lunar satellite orbit) than does the triaxiality perturbation. For example, the earth's contribution to the radial excursion is 0.009 n mi during a 14 day mission. Thus, by neglecting the Earth perturbation, a maximum short period radial excursion error of 0.009 n mi is introduced.

LEM orbital inclination and right ascension of the ascending node long period and secular excursions must also be considered. Reference 4 indicates that for a lunar equatorial satellite the Earth has a more predominant influence on these parameters than does the lunar triaxiality orbit. The reason for this is that, to the first order, there is no lunar triaxiality perturbation normal to the equatorial plane. The Earth perturbation, however, does produce a disturbing force component normal to this plane. Thus, inclination or nodal excursions, for a lunar equatorial orbit, reflect the effect of the Earth's influence rather than the influence of a triaxial Moon.

1132

Although the earth perturbation, on satellite inclination, exceeds that of the Moon, the resultant multibody inclination excursions are still small. For example, the equivalent angular satellite position error due to neglecting the Earth, based on representative initial conditions (low altitude, circular, lunar equatorial orbit), is approximately 0.01 n mi after each satellite revolution. (reference 4). As the LEM orbit inclination with respect to the lunar equator increases, the earth's secular perturbative influence diminishes relative to the lunar triaxiality perturbation. Since the LEM lunar mission is of the order of a few days, and the resultant earth induced excursions are well within "spec limits" (reference 1), the Earth has been deleted as a perturbing body during lunar separation-to-descent and ascent-to-rendezvous mission phases.

4. LEM Equations of Motion. - In the absence of solar and Earth perturbations, the LEM translational equations (a-1) with respect to a Moon centered M-frame become:

$$\ddot{\bar{r}}_{M/L} = \frac{-\mu_M \bar{r}_{M/L}}{r^3_{M/L}} + \bar{P}_{M/L} + \sum \frac{\bar{F}_{M/L}}{m_L} \qquad \text{(A-10)}$$

It remains to determine the expanded form of the triaxiality perturbation and the summation of the external forces acting on the LEM vehicle. Each item is subsequently discussed.

a. Lunar Triaxiality Perturbation. The recommended form of the lunar triaxiality potential is (reference 2):

$$\Phi_M = C\left[A\left(1 - \frac{3Z^2_{S/L}}{r^2_{M/L}}\right) + B\left(1 - \frac{3Y^2_{S/L}}{r^2_{M/L}}\right)\right] \qquad \text{(a-2)}$$

Constants A, B, and C have been determined by a NASA Earth Model Meeting and are given as (reference 2):

$$A = \frac{I_C - I_A}{I_C} = 621.1358 \times 10^{-6}$$

$$B = \frac{I_B - I_A}{I_C} = 207.0881 \times 10^{-6} \qquad \text{(A-01)}$$

33

$$C = \left(\frac{3}{2} \quad \frac{I_C}{m_M \quad R_M^2} \right) \left(\frac{\mu_M R_M^2}{3} \right) = 1.1263979 \times 10^{27} \quad \frac{ft^5}{sec^2}$$

Principal moments of inertia, I_A, I_B, I_C are measured along the Moon's long, intermediate and short axis, respectively.

The triaxiality perturbation acting on the LEM vehicle is given by the gradient of (a-2), thus

$$\bar{P}_S = P_{X_S} \hat{i}_S + P_{Y_S} \hat{j}_S + P_{Z_S} \hat{k}_S$$

where,

$$P_{X_S} = \left(\frac{3CX_{S/L}}{r^5_{M/L}} \right) F_L \quad ; \quad P_{Y_S} = \frac{3CY_{S/L}}{r^5_{M/L}} (F_L - 2B) \quad ;$$

$$P_{Z_S} = \frac{3CZ_{S/L}}{r^5_{M/L}} (F_L - 2A) \qquad \text{(A-21)}$$

where,

$$F_L = A \left[5 \left(\frac{Z_{S/L}}{r_{M/L}} \right)^2 - 1 \right] + B \left[5 \left(\frac{Y_{S/L}}{5_{M/L}} \right) - 1 \right]$$

Equations (A-21), sheet A, represent the component accelerations with respect to selenographic coordinates. LEM coordinates are computed in the M- frame (A-10). It is therefore necessary to transform LEM position coordinates from the M-frame to the selenographic S-frame. This is accomplished by matrix operator a_{ij} (paragraph D, Equations D-10). Hence:

$$\bar{r}_{S/L} = a_{ij} \bar{r}_{M/L}$$

Once having determined the triaxiality accelerations in the S-frame, (A-21), then these accelerations must be transformed to the M-frame; therefore:

$$\bar{P}_M = a_{ij}^T \bar{P}_S \qquad \text{(A-20)}$$

This completes the triaxiality perturbation computations.

b. Main Engine Thrust Forces. - Descent or ascent engine thrust forces (T_k; k = D or A) are supplied by the Propulsion Math Model. The descent engine nozzle is gimballed to provide moment in addition to translational control. Descent engine gimbal angles δ_{θ_D} and δ_{ψ_D} are depicted in Sheet K Figure 2. These angles are generated by the Stabilization and Control Math Model

The ascent engine nozzle is fixed to the body. Angles δ_{θ_A} and δ_{ψ_A} are math model input constants that reflect any angular misalignment between the thrust axis $\hat{T}_A$ and the body axis $\hat{X}_B$. Main engine thrust forces resolved along the body axes take the following form:

$$T_{X_{BK}} = T_K \text{ Cos } \delta_{\psi_K} \text{ Cos } \delta_{\theta_K}$$

$$T_{Y_{BK}} = T_K \text{ Sin } \delta_{\psi_K} \qquad \text{(A-30)}$$

$$T_{Z_{BK}} = T_K \text{ Cos } \delta_{\psi_K} \text{ Sin } \delta_{\theta_K}$$

c. RCS Thrust Forces. - The reaction control system consists of 16 thrusters mounted on support booms in clusters of four as shown in Figure 3. Two separate propellant systems are provided. Unshaded and shaded thruster nozzles correspond to systems "a" and "b", respectively. Each thruster is designated by a number (T_u, u = 1, 2,..16). Translational forces and/or moments are generated by appropriate thrust commands issued from the Reaction Control System math model.

RCS force components along the body axes are:

$$T_{X_{BR}} = T_2 + T_6 + T_{10} + T_{14} - (T_1 + T_5 + T_9 + T_{13})$$

$$T_{Y_{BR}} = T_{12} + T_{16} - (T_4 + T_8) \qquad \text{(A-50)}$$

$$T_{Z_{BR}} = T_7 + T_{11} - (T_3 + T_{15})$$

d. Fuel and Oxidizer Slosh Forces. - Vehicle torques induced by main engine propellant oscillations during the powered descent and ascent maneuvers effect the RCS propellant consumption and limit cycle characteristics (reference 5, 39). Thus, any meaningful math model should have provisions to simulate propellant slosh force and torque perturbations, (see equations A 41, 42, 43, 55).

The model consists of a single pendulum located along the X body axis. The position of the pendulum, its natural frequency and its mass are given as a function of fluid height. The term m_{SKj}, the slosh mass, is the sum of the sloshing masses in each of the four descent or two ascent tanks. The natural frequency ω_{nk}, is calculated using the parameters corresponding to tank #1 for both ascent and descent. The lengths α_{K1}, β_K, and γ_K are the X, Y, Z distances from the vehicle CG to the pendulum pivot.

e. Stage Separation Forces. - Substantial separation forces exist whenever the descent stage is separated from the ascent stage. A detailed derivation of the separation forces are given in reference 9 and will not be repeated herein. Instead, a brief description of the logic flow is presented.

Staging forces are considered as a perturbation to the total thrust and are activated at the instant of ascent engine ignition. Staging forces have a characteristic shape shown in the accompanying sketch (see A-60, 61):

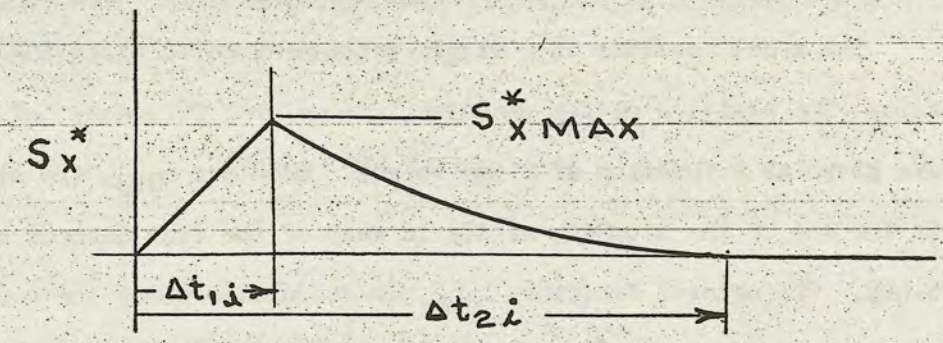

Time measured from Ascent Engine ignition in seconds.

At ascent engine ignition, the stage separation force increases linearly to a maximum value. The thrust decay characteristic is represented by a third order polynomial that has a zero value at time Δt_{2_i}. This polynomial can be represented by a linear decay characteristic without any loss in realism. All stage separation coefficients and timing events depend on whether an abort, with partial (i = PP) or full (i = FP) tank pressure, or a lunar lift-off (i = LO) is being performed (A-61).

f. Non-Gravity Force Summation. - All external, non-gravitational forces are summed in A-81 and transformed from body axes coordinates to inertial M-Frame coordinates in block A-80 for direct use in the equations of motion (A-10).

B. LEM CSM Position Equations and CSM Trajectory

1. Purpose.- The purpose of set B is:

a. To provide LEM and CSM oblateness and aerodynamic perturbations.

b. To describe relative position and motion between the LEM and CSM.

c. Generate 2-Body Kepler parameters for use in the LGC computations.

2. LEM and CSM Equations of Motion.- The basic equation of motion is:

$$\ddot{\bar{r}} = -\frac{\mu}{r^3_{n/v}}\bar{r}_{n/v} + \bar{P}_{n/v} + \bar{A}_v \qquad \begin{matrix} v = L \text{ or } e \\ n = M \text{ or } e \end{matrix}$$

Vector $\bar{P}_{v/N}$ denotes either the moon's triaxialty accelerations (A-20) or the earth's non-central gravitational acceleration B40. The latter is derived from the gradient of the potential function (Φ_v).

The oblateness perturbations can be written as:

$$\ddot{X}'_{E/V} = -\frac{\mu_E (X_E)_V}{r^3_{E/V}}\left\{J\left(\frac{R_E}{r_{E/V}}\right)^2\left\{1-5\left[\frac{(Z_E)_V}{r_E}\right]^2\right\}\right. \qquad B-40$$

$$+3H\left(\frac{R_E}{r_{E/V}}\right)^3\frac{(Z_E)_V}{r_{E/V}}\left\{1-\frac{7}{3}\left[\frac{(Z_E)_V}{r_{E/V}}\right]^2\right\}$$

$$\left.+\frac{3}{7}D\left(\frac{R_E}{r_{E/V}}\right)^4\left\{1-14\left[\frac{(Z_E)_V}{r_{E/V}}\right]^2+21\left[\frac{(Z_E)_V}{r_{E/V}}\right]^4\right\}\right\}$$

$$\ddot{Y}'_{E/V} = -\frac{\mu_E (Y_E)_V}{r^3_{E/V}}\left\{J\left(\frac{R_E}{r_{E/V}}\right)^2\left\{1-5\left[\frac{(Z_E)_V}{r_{E/V}}\right]^2\right\}\right.$$

$$+3H\left(\frac{R_E}{r_{E/V}}\right)^3\left\{\frac{(Z_E)_V}{r_{E/V}}-\frac{7}{3}\left[\frac{(Z_E)_V}{r_{E/V}}\right]^3\right\}$$

$$\left.+\frac{3}{7}D\left(\frac{R_E}{r_{E/V}}\right)^4\left\{1-14\left[\frac{(Z_E)_V}{r_{E/V}}\right]^2+21\left[\frac{(Z_E)_V}{r_{E/V}}\right]^4\right\}\right\}$$

1139

$$\ddot{Z}'_{E/V} = -\frac{\mu_E (Z_E)_V}{r_{E/V}^3}\left\{J\left(\frac{R_E}{r_{E/V}}\right)^2\left\{3-5\left[\frac{(Z_E)_V}{r_{E/V}}\right]^2\right\}\right.$$

$$+H\left(\frac{R_E}{r_{E/V}}\right)^3\left\{6\left[\frac{(Z_E)_V}{r_{E/V}}\right]-7\left[\frac{(Z_E)_V}{r_{E/V}}\right]^3-\frac{3}{5}\left[\frac{r_{E/V}}{(Z_E)_V}\right]\right\}$$

$$\left.+\frac{D}{7}\left(\frac{R_E}{r_{E/V}}\right)^4\left\{15-70\left[\frac{(Z_E)_V}{r_{E/V}}\right]^2+63\left[\frac{(Z_E)_V}{r_{E/V}}\right]^4\right\}\right\}$$

Vehicle aerodynamic accelerations $\bar{A}_V$ (C_D = constant) are:

$$\bar{A}_V = \frac{1}{2}\left[\frac{\rho(hv)\, V_{R/V}^2\, C_{D_V} S_V}{m_V}\right]\frac{\bar{V}_{R/V}}{V_{R/V}} \qquad \text{(B-30, 31)}$$

Where, the velocity of the CSM or LEM relative to a rotating atmosphere is:

$$\bar{V}_{R/V} = \dot{\bar{r}}_{E/V} - \bar{\omega}_E \times \bar{r}_{E/V} \qquad \text{(B-32)}$$

The oblateness terms and the aerodynamic terms are combined to obtain Total Earth Perturbations:

$$\bar{P}_{E/V} = \ddot{\bar{r}}'_{n/V} + A_{n/V} \qquad \text{(B-42)}$$

These are then used in quotion set (A-10) to derive vehicle position and velocity.

3. LEM-CSM Relative Position and Motion - The results of loop A-10 are differenced for the two vehicles thus obtaining relative parameters:

$$\dot{\bar{\rho}}_n = \dot{\bar{r}}_{n/C} - \dot{\bar{r}}_{n/L} \qquad \text{(B-11)}$$

$$\bar{\rho}_n = \bar{r}_{n/C} - \bar{r}_{n/L} \qquad \text{(B-10)}$$

4. Two Body Equations of Motion - The CSM state vector based on a spherical symmetric force field is:

$$\ddot{\bar{r}}_{n/c} = -\frac{\mu_n}{r^3_{n/c}}\,\bar{r}_{n/c} \qquad \text{(b-16)}$$

The solution for central force motion can be written in terms of four scalar parameters (reference 12):

$$\bar{r}_{n/c} = f\,\bar{r}_{n/c_o} + g\,\dot{\bar{r}}_{n/c_o}$$
$$\dot{\bar{r}}_{n/c} = \dot{f}\,\bar{r}_{n/c_o} + \dot{g}\,\dot{\bar{r}}_{n/c_o} \qquad \text{(B-20)}$$

Scalar parameters f, g, $\dot{f}$, $\dot{g}$ (B-26) depend on the instantaneous orbit radius, appropriate orbit constants and the difference in eccentric anomaly ($E-E_o$) measured from epoch (problem start t = 0). The delta eccentric anomaly ($E-E_o$) is computed from Kepler's equation, using a Newton Raphson iteration technique, at any desired interval of time t measured from problem start (see B-25). Thus, CSM motion is known once CSM initial conditions $\bar{r}_{n/c_o}$, $\dot{\bar{r}}_{n/c_o}$ are specified. Subsidiary calculations are performed to define the initial CSM radius, radius rate, velocity and angular momentum components for use in other subset equations.

Equations B-20, in the form shown, will be used as inputs to the LGC during the ascent-to-terminal rendezvous maneuver (see True Motion Equations sheets N, O, P).

1141

C. LEM Rotational Equations of Motion

1. Purpose. - The purpose of Set "C" equations is to accurately represent the rotational dynamics of the LEM vehicle during all LMS mission phases.

2. Rotational Equations. - The standard, rigid-body, rotational equations of motion are given by equations C-10. These equations are written with respect to a non-principal, body axis system located at the instantaneous C.G. Body axes X_B, Y_B, Z_B, are oriented parallel to the symmetry axes as shown in Figures 3 and 4. The more important time derivative moment of momentum terms, representing fluid particle motions (fuel slosh) and particles being transferred out of the system (damping), are combined into the moment components L_B, M_B, and N_B. Instantaneous moments and products of inertia are generated in paragraph III-I, titled, Weights and Balance. Product of inertia terms are retained to account for off-load conditions resulting, for example, from a fuel or oxidizer leak or pump malfunction.

Equations C-11 are the first integrals of equations C-10 and represent inertial angular rates p_B, q_B, r_B about the vehicle X_B, Y_B, and Z_B directions, respectively.

3. External torques.

a. RCS Torques. - Equations (C-51) define the RCS torques with respect to a fixed reference point. This point lies in the RCS plane of symmetry at distances l_1, and l_2 measured from the inner and outer thruster arms (Figure 3). Moments about the fixed reference point are subsequently transferred to the vehicle CG (C-50), which is displaced from the reference point by component distances

* $\bar{\alpha}_R, \bar{\beta}_R, \bar{\gamma}_R$ along body axes X_B, Y_B, Z_B. Transferring the moments, rather than computing the moments directly about the CG, results in algebraic simplification.

b. Main Engine Torques. - Thrust components resulting from descent engine gimbal nozzle action or ascent engine misalignment have been ascertained (A-30). The moment arm from the nozzle throat to the vehicle CG is computed by subset equation I-30:

$$\bar{d}_K = \bar{\alpha}_K \hat{\imath} + \bar{\beta}_K \hat{\jmath} + \bar{\gamma}_K \hat{k} \qquad \text{(c-1)}$$

Hence, the total amount about the CG is:

$$\bar{M}_K = \bar{d}_K \times \bar{T}_{BK} \qquad \text{(C-30)}$$

which leads to equation C30.

c. Fuel Slosh Torques. - The slosh moments (C-40), are defined by the perturbative slosh forces (A-41) and their corresponding distances $\bar{\alpha}_{K_l}$ & $\bar{\gamma}_{K_l}$, measured from the tank centroid to the composite vehicle CG.

---

* Bars in this instance do not represent vectors but component distances measured from the instantaneous CG.

1147

11/65

d. Engine Separation Torques. - Present indications are that the stage separation torque perturbations (references 9 and 22) are large and cannot be neglected. Furthermore, the moment arm relating the position of force application to the vehicle CG is a time dependent variable. For this reason, the moment perturbations (C-60) are not represented by a constant arm times the stage separation force (equations A-60). The moment time transient, however, has a shape similar to the stage separation force profile.

Should future refined studies indicate a small moment arm variation with time, then stage separation torques could be computed using an average, constant moment arm times the stage separation force (A-60).

e. Moment Summation. All external LEM torques are summed in subset (C-80) for insertion into the rotational equations of motion.

During the integrated mode, in the docked configuration, both the LMS and the AMS will solve the rotational equations of motion. This requires that the AMS provide CSM external torques (C-81) relative to the LEM body axis about the composite LEM-CSM center of mass. When docked, the LEM $\hat{X}_B$ axis is directed opposite to the CSM $\hat{X}_B$ axis. An arbitrary fixed roll angle ($\phi+\phi_c$) may exist between the LEM and CSM $\hat{Y}_B$ axis.

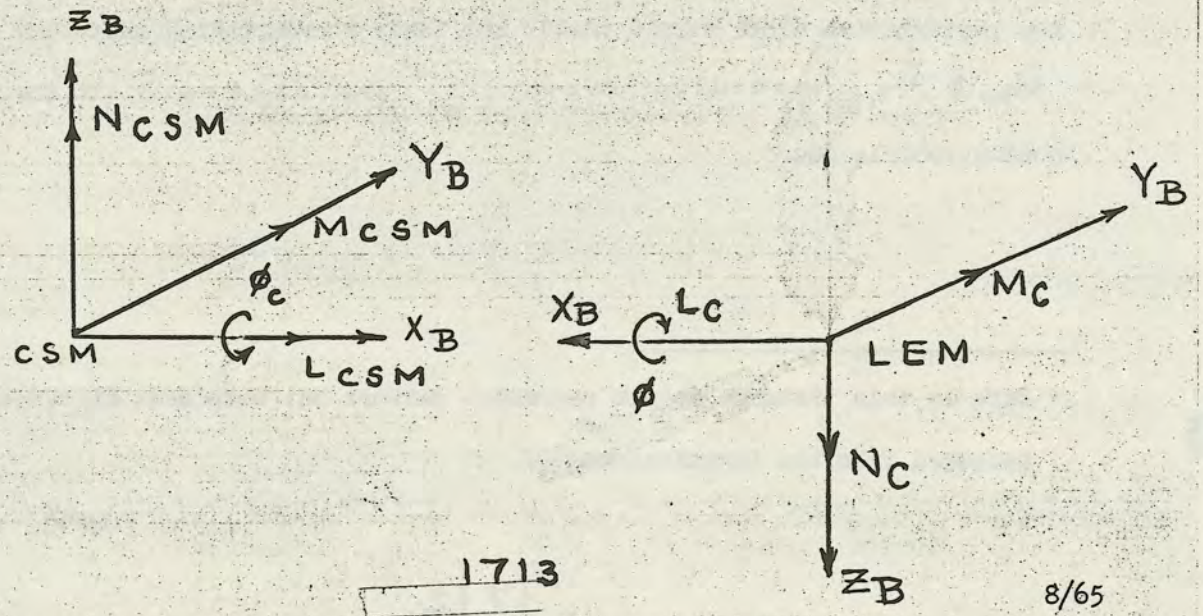

CSM external torques (L_{csm}, M_{csm}, N_{csm}) computed by the AMS relative to the CSM body axis are transformed as follows prior to insertion into (C-10).

$$L_c = -L_{csm}$$

$$M_c = M_{csm}\cos(\phi_c + \phi) - N_{csm}\sin(\phi_c + \phi)$$

$$N_c = -N_{csm}\cos(\phi_c + \phi) - M_{csm}\sin(\phi_c + \phi)$$

4. LEM Orientation Computations

a. General. - Basic to all rigid body simulation problems is the specification of vehicle orientation with respect to a known coordinate reference.

The coordinate reference selected, for purpose of the LMS simulation, is the inertial M or E - frame rather than the true I M U reference frame. This choice is made to simplify the LMS - AMS interface requirements and to prevent erractic visual display motion wherever the true reference frame, computed within the L G C, is altered.

Vehicle orientation is simulated by integrating the rotational equations of motion to obtain body rates p_B, q_B, r_B. Once body rates are obtained (C-11), then the time dependent direction cosine matrix can be generated from either:

i. the Euler rate equations $(\dot{\theta}, \dot{\psi}, \dot{\phi})$.

ii. the direction cosine rate equations $(\dot{a}_{ij};\ i = 1,2,3;\ j = 1,2,3)$.

iii. the quaternion rate equations $(\dot{e}i;\ i = 1, 2,3,4)$.

Euler rate equations are simple to implement; however, these equations introduce inaccuracies as the middle angle or second ordered rotation approaches. $\pm \frac{\pi}{2}$. This condition is normally referred to as "gimbal lock." In a gimbal lock configuration, the inner and outer rotation axes coincide resulting in infinite inner and outer angular rates. Euler rate equations are inappropriat-

1145

for mechanization since an all attitude capability is desired for complete LEM simulation. Resort to an analytic description of a redundant four gimbal set is not considered because of unwarranted complexity.

The direction cosine rate equations and the quaternion rate equations do not exhibit any singularities. It remains, therefore, to determine which of these two techniques are best suited for LMS mechanization.

b. Selection Criteria. - An empirical study (references 23, 24 and 25) was conducted on the 7094 digital computer to ascertain the relative advantage between using either direction cosine or quaternion rate equations to define vehicle orientation angles for digital simulation. The relative advantage of each technique was evaluated by comparing computer storage requirements, solution speed and Euler angle output accuracy for a variety of numerical integration schemes and integration intervals. Accuracy comparisons were made by matching digital outputs to an analytical Euler angle solution for coning motion. Study results indicated that the quaternion rate equations were slightly superior in all categories. Hence, the quaternion rate equations given below, will be mechanized for simulation (reference 26):

$$\dot{e}_1 = \frac{1}{2}\left(-e_4 p_B - e_3 q_B - e_2 r_B\right)$$

$$\dot{e}_2 = \frac{1}{2}\left(-e_3 p_B - e_4 q_B + e_1 r_B\right) \qquad \text{(C-20)}$$

$$\dot{e}_3 = \frac{1}{2}\left(e_2 p_B + e_1 q_B - e_4 r_B\right)$$

$$\dot{e}_4 = \frac{1}{2}\left(e_1 p_B - e_2 q_B + e_3 r_B\right)$$

c. Euler Angle Matrix Operator.- Physically, parameters e_i represent trigonometric functions of three direction cosines and a rotation angle. The three direction cosines position a rotation axis about which the rotation angle carries the rigid body from an arbitrary initial orientation to an arbitrary final orientation. Starting values for e_1, e_2, e_3 and e_4 are required in order to initialize (C-20). In addition, the inverse problem of specifying a body axes orientation, given instantaneous values of e_i, must also be defined. Initial e_i values are not known directly since it is assumed that the LEM vehicle orientation will be given in terms of Euler angles θ, ψ and ϕ. Thus, the correspondence between the four parameter set and the Euler angle set must be ascertained. Prior to defining this correspondence, it is first necessary to define the LEM Euler angles.

LEM Euler angles are specified by a specific sequence of ordered rotations which differ from standard aircraft usage. The transformation from the reference axes (X_n, Y_n, Z_n) to the body axes (X_B, Y_B, Z_B) is given by the following ordered counterclockwise rotations:

i. Pitch (θ) about the Y_n reference axis.

ii. Yaw (ψ - pilot roll) about the new Z' axis so formed.

iii. Roll (ϕ - pilot yaw) about the new X" axis so formed to give X_B, Y_B, Z_B directions.

The foregoing rotations are represented in matrix form as follows:

$$\bar{r}_B = g_{ij_n} \bar{r}_n \qquad \text{(D-40)}$$

where:

$$g_{ij} = \begin{Bmatrix} g_{11} & g_{12} & g_{13} \\ g_{21} & g_{22} & g_{23} \\ g_{31} & g_{32} & g_{33} \end{Bmatrix}$$

and where:

1147

$$g_{ij} \begin{Bmatrix} \cos\phi\cos\theta & \sin\psi & -\cos\psi\sin\theta \\ -\cos\phi\sin\psi\cos\theta + \sin\phi\sin\theta & \cos\phi\cos\psi & +\cos\phi\sin\psi\sin\theta + \sin\phi\cos\theta \\ \sin\phi\sin\psi\cos\theta - \cos\phi\sin\theta & -\sin\phi\cos\psi & -\sin\theta\sin\phi\sin\psi + \cos\phi\cos\theta \end{Bmatrix} \quad (C\text{-}5)$$

It must be mentioned that the Euler angles θ, ψ, ϕ described are not used to orient the astronauts "8-Ball" display. The "8-Ball" display is activated by indicated Euler angles θ_{IMU} and ϕ_{IMU} (sheet L). These indicated angles correspond to gimbal pickoff resolvers and reflect the LEM body orientation with respect to the physical "on-board" platform.

d. Quaternion Initialization. - It can be shown (references 26 and 27), that for each real, three-dimensional, orthogonal transformation matrix (c-5) there is an associated two by two imaginary matrix that relates the initial vehicle orientation to the final vehicle orientation. The complex matrix must; a) be unitary, the product of the matrix and the transpose of its complex conjugate is unity, and b) have a determinant = +1. These conditions lead to the following operator form:

$$H = \begin{pmatrix} e_1 + ie_2 & e_3 + ie_4 \\ -e_3 + ie_4 & e_1 - ie_2 \end{pmatrix} \quad (c\text{-}6)$$

Real numbers e_i are the quaternions or Euler Parameters.

Proof is given in reference 26 that the following similarity transformation;

$$P' = H(P)(H)^{-1} \quad (c\text{-}7)$$

$$P = \begin{pmatrix} Z & X - iy \\ x + iy & -Z \end{pmatrix}$$

satisfies all the requirements of a real orthogonal transformation operator when X, Y, and Z are interpreted as vector components. Substituting (c-6) into (c-7) and expanding gives:

$$\bar{r}_B = g_{ijn}\,\bar{r}_n \quad (D\text{-}40)$$

$$g_{ij} = \begin{Bmatrix} e_1^2-e_2^2-e_3^2+e_4^2 & 2(e_1e_2+e_3e_4) & 2(e_2e_4-e_1e_3) \\ 2(e_3e_4-e_1e_2) & e_1^2-e_2^2+e_3^2-e_4^2 & 2(e_2e_3+e_4e_1) \\ 2(e_1e_3+e_2e_4) & 2(e_2e_3-e_1e_4 & e_1^2+e_2^2-e_3^2-e_4^2 \end{Bmatrix}$$

Only three of the four quaternions are independent. The fourth is related to the other three by the equation:

$$e_1^2+e_2^2+e_3^2+e_4^2 = 1 \qquad \text{(c-8)}$$

This dependency forms the basis of a rectification scheme which is used to maintain direction cosine orthonormality (reference 28).

Consider the first ordered rotation θ about Y_n ($\psi = \phi = 0$). There must be a one-to-one correspondence between matrix operator g_{ij} (c-5) and matrix operator g_{ij} (D-40). Comparing elements of each matrix gives:

$$\begin{aligned} e_1^2-e_2^2-e_3^2+e_4^2 &= \cos\theta \\ 2(e_3e_4-e_1e_2) &= 0 \\ 2(e_1e_3+e_2e_4) &= \sin\theta \\ 2(e_1e_2+e_3e_4) &= 0 \\ e_1^2-e_2^2+e_3^2-e_4^2 &= 1 \\ 2(e_2e_3-e_1e_4) &= 0 \\ 2(e_2e_4-e_1e_3) &= -\sin\theta \\ 2(e_2e_3+e_4e_1) &= 0 \\ e_1^2+e_2^2-e_3^2-e_4^2 &= \cos\theta \end{aligned} \qquad \text{(c-9)}$$

Set (c-9) is satisfied if any only if:

$$e_2 = e_4 = 0 \qquad \text{(c-10)}$$

whereupon elements (c-9) reduce to:

1149

$$e_1 = \frac{\sin\theta}{2\sin\theta/2} = \cos\theta/2$$
$$e_3 = \sin\theta/2 \qquad \text{(c-11)}$$

But, it was indicated earlier that complex matrix H (c-6) represents a real rotation. Hence, substituting elements (c-10) and (c-11) into (c-6) gives:

$$H_\theta = \begin{pmatrix} \cos\theta/2 & \sin\theta/2 \\ -\sin\theta/2 & \cos\theta/2 \end{pmatrix} \qquad \text{(c-12)}$$

Repeating this procedure for the second ordered rotation (ψ) and the third ordered rotation (ϕ) yields:

$$H_\psi = \begin{pmatrix} \cos\psi/2 + i\sin\psi/2 & 0 \\ 0 & \cos\psi/2 - i\sin\psi/2 \end{pmatrix} \qquad \text{(c-13)}$$

$$H_\phi = \begin{pmatrix} \cos\phi/2 & i\sin\phi/2 \\ i\sin\phi/2 & \cos\phi/2 \end{pmatrix} \qquad \text{(c-14)}$$

The final vehicle orientation, resulting from θ, ψ and ϕ rotations, is specified by rotation matrices c-12, c-13, c-14:

$$H = \begin{pmatrix} e_1 + ie_2 & e_3 + ie_4 \\ -e_3 + ie_4 & e_1 - ie_2 \end{pmatrix} = H_\phi H_\psi H_\theta \qquad \text{(c-15)}$$

Expanding the right hand member of (c-15) and comparing each element to the left hand member gives the desired result:

$$e_{10} = \text{COS}\ \phi_o/2\ \text{COS}\psi_o/2\ \text{COS}\ \theta_o/2 - \text{SIN}\ \phi_o/2\ \text{SIN}\psi_o/2\ \text{SIN}\ \theta_o/2$$
$$e_{20} = \text{COS}\ \phi_o/2\ \text{SIN}\psi_o/2\ \text{COS}\ \theta_o/2 - \text{SIN}\ \phi_o/2\ \text{COS}\psi_o/2\ \text{SIN}\ \theta_o/2$$
$$e_{30} = \text{COS}\ \phi_o/2\ \text{COS}\psi_o/2\ \text{SIN}\ \theta_o/2 + \text{SIN}\ \phi_o/2\ \text{SIN}\psi_o/2\ \text{COS}\ \theta_o/2$$
$$e_{40} = \text{COS}\ \phi_o/2\ \text{SIN}\psi_o/2\ \text{SIN}\ \theta_o/2 + \text{SIN}\ \phi_o/2\ \text{COS}\psi_o/2\ \text{COS}\ \theta_o/2 \qquad \text{(C-21)}$$

Equations (C-21) are used once during each run. They specify the quaternions at problem start based on known initial values of the LEM Euler angles with respect to the inertial M, or E-frame.

e. Inverse Problem. - Direction cosine matris elements g_{ij} (D-40) are known at each instant of time. It is desired to determine the corresponding Euler angles to use as drive inputs for gimballed visual displays (see for example J-10, J-41, and J-60). As mentioned earlier each element of (D-40) must be identical to each element of (C-5). With regard to the first ordered rotation, Θ, it is seen that:

$$\text{Tan}\Theta = \frac{-(-\sin\Theta\cos\psi)}{\cos\Theta\cos\psi} = \frac{-g_{13}}{g_{11}} \qquad \text{(c-16)}$$

The middle rotation ψ could be defined as:

$$\text{Sin}\,\psi = g_{12} \qquad \text{(c-17)}$$

or:

$$\text{Tan}\,\psi = \frac{\sin\psi}{(\cos\psi\cos\Theta)\cos\Theta-(-\cos\psi\sin\Theta)\sin\Theta} \qquad \text{(c-18)}$$

$$= \frac{g_{12}}{g_{11}\cos\Theta - g_{13}\sin\Theta}$$

Similarly, the outer rotation angle could be given by:

$$\text{Tan}\phi = \frac{-(-\sin\phi\cos\ )}{\cos\phi\cos\psi} = \frac{-g_{32}}{g_{22}}. \qquad \text{(c-19)}$$

or:

$$\text{Tan}\,\phi = \frac{(-\text{Cos}\,\phi\,\text{Sin}\quad\text{Cos}\,\Theta + \text{Sin}\,\phi\,\text{Sin}\,\Theta)\,\text{Sin}\,\Theta + (\text{Cos}\,\phi\,\text{Sin}\quad\text{Sin}\,\Theta + \text{Sin}\,\phi\,\text{Cos}\,\Theta)\,\text{Cos}\,\Theta}{(\text{Sin}\,\phi\,\text{Sin}\quad\text{Cos}\,\Theta - \text{Cos}\,\phi\,\text{Sin}\,\Theta)\,\text{Sin}\,\Theta + (-\text{Sin}\,\phi\,\text{Sin}\quad\text{Sin}\,\Theta + \text{Cos}\,\phi\,\text{Cos}\,\Theta)\,\text{Cos}\,\Theta}$$

$$= \frac{g_{21} \sin\theta + g_{23} \cos\theta}{g_{31} \sin\theta + g_{33} \cos\theta} \qquad (20)$$

Equations c-16, c-17 and c-19 have obvious advantages. However, as ψ approaches $\pm \frac{\pi}{2}$, θ and ϕ are undefined. This is not consistent with the requirement of an "all attitude capability."

"Gimbal lock" can be artificially circumvented by applying the following logic to equations c-16, c-18, and c-20. As the middle rotation (ψ) approaches $\pi/2$ (say $\pi/2 \pm \epsilon^*$), freeze θ at its current value, but continue to compute ϕ. This technique will ensure that the sum $\theta + \phi$ is correct to order ϵ^*. Realize that in the neighborhood of $\psi = \pm \pi/2$, the inner and outer rotation axes are nearly coincident, therefore, the sum $\theta + \phi$ is sufficient to specify a true vehicle space orientation. Gimbal lock logic is not required whenever ψ leaves the neighborhood given by $\pi/2 \pm \epsilon^*$, since algebraic equations c-16, c-18, c-20 are self sufficient.

D. GENERAL TRANSFORMATIONS

1. Purpose. - The purpose of Set D is to generate the more important transformation relationships used in the LMS Math Model. The transformation operators listed below, are derived in this subsection.

Matrix Operator	Transforms any Vector measured in the:	To the:	As follows:
a_{ij}	Inertial Lunar M-Frame	Selenographic S - Frame.	$\bar{r}_S = a_{ij}\,\bar{r}_M$
c_{ij_E}	Inertial Earth E-Frame	True IMU reference R-Frame.	$\bar{r}_R = C_{ij_E}\,\bar{r}_E$
c_{ij_M}	Inertial Lunar M-Frame.	True IMU reference R-Frame.	$\bar{r}_R = C_{ij_M}\,\bar{r}_M$
g_{ij_n}	Inertial M or E-Frame.	LEM Gody B-Frame.	$\bar{r}_B = g_{ij_n}\,\bar{r}_n$
f_{ij}	Inertial Earth E Frame.	Rotating Geographic G - Frame.	$\bar{r}_G = f_{ij}\,\bar{r}_E$
l_{ij_n}	Window or telescope optical pg-frame	Inertial Earth E, or Moon-M Frame	$\bar{r}_n = l_{ijn}\,\bar{r}_{pq}$

2. Matrix Operator From Inertial M - Frame to Selenographic S - Frame. - During lunar missions it is essential to position the inertial platform, define the trajectory and provide visual cues with sufficient realizm relative to known lunar landmarks. An accurate representation of the Moon's motion is required to accomplish this task.

Let the selenographic Z_s axis be defined by the Moon's rotation vector. Neglecting physical librations, axis $\hat{Z}_s$ makes a constant angle of 1° 32.1' (Hayn's constant) with the ecliptic Northpole. Based on Cassini's laws (reference 29), the pole of the Moon's orbit P describes a small circle about the ecliptic pole in about 18.6 years. The great circle arc $\widehat{Z_s P}$ contains the ecliptic pole, which lies between $\hat{Z}_s$ and $\hat{P}$. Thus, the lunar equator and the lunar orbit have a common line of nodes with respect to the ecliptic. Define the $\hat{X}_s$ axis to lie along the Moon - Earth line when the Moon is at the ascending node and concurrently at either apogee or perigee (reference 29). Ordered rotations necessary to establish the time dependent relationship between this fixed selenographic frame and the basic computational mean equinox, mean equator of date reference system is discussed next.

Refer to Figure 6. Rotate about the mean equinox $\hat{X}_M$ through the mean obliquity, ϵ. This establishes the ecliptic system:

$$\bar{r}_\epsilon = a_{mj}\, \bar{r}_M \qquad \text{(D-16)}$$

Next, establish the Moon's mean ascending node by a rotation (Ω) about the ecliptic pole:

$$\bar{r}_\Omega = a_{mn}\, \bar{r}_\epsilon \qquad \text{(D-14)}$$

From Cassini's laws, the ascending node of the lunar orbit defines the descending node of the lunar equator. A clockwise rotation (I) about the node through Hayn's constant locates the lunar equator relative to the ecliptic plane:

$$\bar{r}_I = a_{lm}\, \bar{r}_\Omega \qquad \text{(D-15)}$$

Neglecting physical librations, the prime lunar meridian, which lies in the $\hat{X}_s - \hat{Z}_s$ plane and faces the earth, rotates at a rate equivalent to the Moon's mean motion. At any instant therefore, the prime meridian is at an angular distance of $\pi + (\ell - \Omega)$ measured from the mean ascending lunar orbit node. Symbol ℓ represents the mean lunar longitude. The final rotation operator is:

$$\bar{r}_{S\,MEAN} = a_{kl}\,\bar{r}_I \qquad \text{(D-13)}$$

Combining equations D-13 through D-16 gives the transformation from the inertial M-frame (fixed at problem start) to a non-nutating, selenographic S-frame:

$$\bar{r}_{S\,MEAN} = a_{kl}\,a_{ln}\,a_{mn}\,a_{nj}\,\bar{r}_M \qquad \text{(d-1)}$$

Equation (d-1) does not reflect the complex wobbling motion of the Moon, normally referred to as physical libration. Physical libration represents lunar oscillations which have total amplitude variations constrained to $\pm 0.04^\circ$ and associated short and long period motions of 1 and 6 years, respectively. A first order description of this motion is given by the physical libration matrix presented below (references 29 and 30):

$$\bar{r}_S = L_{ik}\,\bar{r}_{S\,MEAN} \qquad \text{(D-11,12)}$$

The desired orientation of the selenographic axis relative to the inertial M-frame is found by substituting (d-1) into (D-11, 12):

$$\bar{r}_S = a_{ij}\,\bar{r}_M \qquad \text{(D-10)}$$

The libration matrix and operator (D-16) have an insignificant variation during the course of any training session. It is therefore recommended that these matrix operators be computed at problem start and maintained constant during any particular run.

3. Matrix Operator From True IMU R-Frame To Inertial E or M-Frame

a. Earth Mission. - At present, the desired LEM platform directions required for earth training exercises are not known. It is arbitrarily assumed that the LEM platform will be referenced to the Earth launch site at launch. Let this position be specified by a known Universal Time measured in hours, H (E-01) from Greenwich Midnight to problem start and integer days. D* (E-01) from Greenwich Midnight Dec. 31, of the launch year to Greenwich Midnight of the launch day. These constants define the Greenwich Hour Angle relative to the mean equinox of date (see loops E-01 and E-10). The position of the launch site at launch is:

$$RA_E = GHA_E + \lambda_E \qquad \text{(D-21)}$$

Parameter λ_E denotes the launch site longitude measured Eastward from Greenwich. The assumed platform direction is space fixed and can now be found by the following three ordered rotations:

i. Rotate about the mean spin axis $\hat{Z}_E$ through RA_E.

ii. Rotate about the new $\hat{Y}_E$ axis so formed through the launch site declination δ_E (positive North).

iii. Rotate about the new $\hat{X}''_E$ axis so formed through the intended launch azimuth angle ψ_E (measured positive East of North), to give assumed Earth mission platform directions $\hat{X}_R$, $\hat{Y}_R$, $\hat{Z}_R$.

The ordered rotations specify the transformation:

$$\bar{r}_{RE} = C_{ij_E}\ \bar{r}_E \qquad \text{(D-20)}$$

b. Lunar Mission.- The desired platform orientation, for all lunar mission modes, is based on references 31 and 32. These references state that the X_R platform axis will be directed from the Moon's center to the intended landing site at some nominal landing time, or take-off site at some nominal take-off time. Moreover, the Z_R platform axis shall parallel to the CSM orbit plane in the direction of motion. A precise definition follows.

Consider a hypothetical mission. Assume CSM-LEM lunar injection has taken place and that the CSM platform is inertially aligned to the M-frame (or E-frame). Subsequent to separation, both LEM and CSM platforms must be aligned to new desired reference directions. These directions are specified by the desired landing site selenographic longitude (λ_S) and latitude (ϕ_S) as well as the desired nominal touchdown time, t*, measured from problem start to touchdown. Time t* specifies the inertial position of the Moon, and hence the landing site, at the nominal time of landing. This landing site position is fixed by:

i. Computing ahead to ascertain the Julian date t* (E-01), and days from epoch d* (E-22) to touchdown.

ii. Computing the lunar and solar orbit elements based on future times t* and d* (E-22).

iii. Using elements (E-20) to compute the transformation matrix a_{ij*} at times t* and d*.

Transformation matrix a_{ij*} specifies the inertial orientation of of the Moon at the nominal touchdown time t*. The landing site unit vector measured in selenographic coordinates is know:

$$\hat{r}_S = \cos\phi_S \cos\lambda_S \hat{i}_S + \cos\phi_S \sin\lambda_S \hat{j}_S + \sin\phi_S \hat{k}_S \qquad \text{(D-33)}$$

Thus, the components of $\hat{r}_S$ transformed to M-frame coordinates correspond exactly to the components of reference direction $\hat{X}_R$ measured in the M-frame:

$$\hat{X}_R = C_{11}\,\hat{i}_M + C_{12}\,\hat{j}_M + C_{13}\,\hat{k}_M = a^*_{ij}\,\hat{r}_M \qquad \text{(D-32)}$$

Reference direction Z_R is parallel to the CSM orbit plane (references 31, 32). This direction is formed by the cross product of the CSM specific angular momentum ($\hat{H}_{M/C}$) and $\hat{X}_R$. Orbit determination techniques will be employed to define the CSM orbit prior to the separation maneuver; consequently, $\hat{H}_{M/C}$ is assumed known:

$$\hat{H}_{M/C} = b'_{21}\,\hat{i}_M + b'_{22}\,\hat{j}_M + b_{23}\,\hat{k}_M \qquad \text{(D-35)}$$

Whereupon reference direction Z_R is:

$$\hat{Z}_R = \frac{\hat{H}_{M/C} \times \hat{X}_R}{\left| \hat{H}_{M/C} \times \hat{X}_R \right|}$$

or:

$$\hat{Z}_R = C_{31}\,\hat{i}_M + C_{32}\,\hat{j}_M + C_{33}\,\hat{k}_M \qquad \text{(D-30)}$$

Orthogonality forces $\hat{Y}_R$: (d-30)

$$\hat{Y}_R = \hat{Z}_R \times \hat{X}_R$$

Combining the foregoing gives the desired transformation matrix:

$$\bar{r}_{RM} = C_{ij}\,\bar{r}_M \qquad \text{(D-30)}$$

Matrix C_{ij} is stored in the LGC computer and subsequently used to align the physical platform (see sheet Q).

The LEM Platform is realigned prior to take-off. Once again, directions $\hat{X}_R$, $\hat{Y}_R$ and $\hat{Z}_R$ are found, given the selenographic latitude and longitude of the take-off site and a nominal take-off time t* measured from problem start. Time t* is given by the allowable launch window variation which in turn is defined during prelaunch operations (see Sheet N).

158

8/65

4. Matrix Operator From Inertial M or E Frame to LEM body B-Frame

The transformation matrix d_{ij} (D-40) has been defined in paragraph 1-3-III-C-4. This matrix is used to define all required LEM body orientations and to position the visual displays.

Transformation matrix d_{ij} and the constant transformation matrix C_{ij} are used to relate the M or E-frame to the LEM body axis:

$$\bar{r}_B = g_{ijn}\, \bar{r}_n \qquad \text{(D-40)}$$

5. Matrix Operator From Inertial E - Frame to Geographic G - Frame

Subset equations (D-60) relate the Greenwich meridian to the E-frame and are used to:

i. Specify the line-of-sight communication requirements between the LEM vehicle and each Earth tracking station.

ii. Position the mission effects projector (MEP) during Earth training exercises.

The Earth's mean equator is defined by the $\hat{X}_E$ - $\hat{Y}_E$ reference plane. consequently, a single rotation about the Earth's mean spin axis ($\hat{Z}_E = \hat{Z}_G$) is sufficient to position the prime meridian relative to the E-frame.

6. Matrix Operator From the LEM Body B-Frame to the Optical Window W-Frame Or Telescope T-Frame

a. General.- Lunar landmarks, the Earth, the CSM, and star positions are observed by the astronauts through either two forward windows, an upper window or one of three telescope positions. Window and telescope optical axes ($\hat{Z}_{pq}$) are shown schematically in Figure 7. Each optical axis has a fixed direction relative to the body axes. For each viewing mode, this direction extends from the flight station design eye to the center of each respective viewing device. All visual displays are positioned relative to this line-of-sight direction. Field of view constraints are automatically included in all visual displays.

8/65

1159

Window and telexcope transformations are generalized by use of dummy subscript pq. Subscript p denotes the viewing device, either window (p = W) or telescope (p = T). Subscript q denotes the viewing mode, either left (q = l), right (q = r) or above (q = a). The generalized transformation matrix given below is based on ordered, right hand rotations specified by input constants ϕ_{pq}, θ_{pq}, ψ_{pq} (see J-01):

$$\bar{r}_{pq} = (h_{ij})_{pq} \bar{r}_B \qquad \text{(D-70)}$$

b. Window Transformations. - The left hand window coordinate axes are derived as follows. Displace the body area from the vehicle CG to the flight station design eye. Rotate about X_B through $+\phi_{Wl}$. Rotate about the new Y_B' axis so formed through a negative angle $-\theta_{Wl}$. This positions the left window axis frame X_{Wl}, Y_{Wl}, Z_{Wl}.
Note that $\psi_{W_q} = 0$.

A similar procedure is repeated for the right window. A negative rotation $-\phi_{Wr}$ is followed by a negative rotation $-\theta_{Wr}$.

Only one rotation is required to specify the above window optical axes, namely, a positive rotation about Y_B through θ_{Wa}.

c. Telescope Transformations. - The center or above telescope axes are given by a single rotation $+\theta_{Ta}$ about the Y_B axis. Three rotations, however, are required to specify the left or right telescope axes relative to the body axes. Consider the left telescope. Axes X_{Tl}, Y_{Tl}, Z_{Tl} are defined by a positive rotation ϕ_{Tl} about X_B, followed by $+\theta_{Tl}$ about Y_B', followed by $-\psi_{Tl}$ about Z_B. The latter transformation is necessary to synthesize prism rotation whenever the Alignment Optical Telescope is slewed. Right telescope ordered rotations are $-\phi_{Tr}$, $+\theta_{Tr}$, $+\psi_{Tr}$.

The optical axes can be transformed directly in M or E-frame coordinates by employing known matrix operators D-70 and D-50.

8/65

Hence:

$$\mathcal{F}_n = (l_{ij})_{pqn}\, \mathcal{F}_{pq} \qquad \text{(D-80)}$$

where:

$$(l_{ij})_{pqn} = (g_{ik})^{T}_{n}\, (h_{kj})^{T}_{pq}$$

Additional transformations, when required for particular subsystem applications, will be discussed in the paragraphs that follow.

E. Ephemeris

1. Purpose.-The purpose of Set E is to define the Moon and Sun positions in mean Earth equator of date coordinates (E-frame), determine the Moon's orbital elements, and generate the Greenwich Hour Angle. Lunar and solar coordinates will be supplied by Jet Propulsion Laboratory (JPL) Ephemeris Tapes (reference 33).

2. Problem Start Initialization.

a. Time.- The JPL tapes are referenced to a 1950.0 epoch and require Julian Date inputs at problem start. It is assumed that training exercises will be initialized by the specification of Universal Time measured in hours H, and days D* of the launch year. Thus, these data must be transformed to Julian Days. This may require counting the number of mean solar days from epoch January 1, 4713 B.C. to problem start.

Consider a reference epoch of 1950.0 (midnight December 31, 1949). Excluding leap years, the number of days from this epoch to problem start is $365\ (Y - 1950) + D^* + \frac{H}{24}$. Leap year days, during the time span (Y-1950), are determined by integer N, where:

$$N = \text{integer value of } 1 + \frac{Y - 1953}{4} \qquad \text{(E-01)}$$

The total number of days from the reference epoch can now be found:

$$d_o = 365\ (Y - 1950) + D^* + \frac{H}{24} + N \qquad \text{(E-01)}$$

Having defined d_o, Julian time measured in terms of Julian centuries from epoch 1950.0 is simply:

$$T_o = \frac{d_o}{36{,}525}$$

This time is fixed at problem start and does not vary during the length of any training mission.

Julian days, measured from January 1, 4713 B.C. to date, are given by equation E-22. This number may be required as an input to the JPL program.

b. Greenwich Hour Angle. The right ascension of the mean sun, corrected for aberration and referenced to the mean equinox of 1950.0, was obtained from reference 16 and is given by subset equation E-10. The Sun's meridian at problem start is employed to specify the time varying Greenwich meridian with respect to the fixed mean equinox of date (E-10).

3. Lunar-Solar Positional and Orbital Elements. The position coordinates of the Moon, $r_{E/M}$, and sun, $r_{E/\odot}$, relative to the mean equinox of date are outputs of the JPL ephemeris program. Therefore, subset equations E-30 and E-31 should not be programmed.

Lunar orbital elements (Ω, ℓ, Γ'), and solar elements (ϵ, $g_\odot$) were obtained from reference 34 and updated from epoch January 0.5, 1900 to reference epoch 1950.0. These elements are given by E-20. They are employed to define the selenographic transformation matrix a_{ij}. Also included is the Moon's mean longitude rate $\dot{\ell}$, which is employed later to define the linear velocity of the LEM's subsatellite point.

F. Rendezvous Radar.

1. Purpose.- The purpose of Set F is to define the line-of-sight vector, measured from the LEM to the CSM, in LEM body coordinates and to provide required inputs to the Rendezvous Radar Subsystem Math Model.

2. Relative Range and Velocity Vectors Measured In LEM Body Axes.

a. Scalar Range and Range Rate. Scalar range defines the linear CG-to-CG distance between the LEM and CSM vehicles:

$$\rho_{LS} = +\sqrt{\rho_{XM}^2 + \rho_{YM}^2 + \rho_{ZM}^2} \qquad \text{(F-10)}$$

Scalar range rate denotes the relative separation or closing speed between the vehicles and is given by:

$$\dot{\rho}_{LS} = \frac{\bar{\rho} \cdot \dot{\bar{\rho}}}{|\bar{\rho}|} = \frac{d}{dt}\sqrt{\rho_X^2 + \rho_Y^2 + \rho_Z^2} = \frac{\rho_X \dot{\rho}_X + \rho_Y \dot{\rho}_Y + \rho_Z \dot{\rho}_Z}{\rho_{LS}} \qquad \text{(F-10)}$$

Parameter $\dot{\rho}_{LS}$ is a required rendezvous and docking display input.

b. M or E-Frame Relative Components.- Component distances and velocities must be ascertained in order to activate equations (F-10). These data are computed from two separate sources. As mentioned in paragraphs A and B, LEM motion is generated with respect to either the inertial M-frame or a non-rotating, but accelerated, relative frame centered at the CSM.

CSM motion is supplied in M-frame coordinates regardless of whether the mission mode is integrated or independent. Accordingly, CSM motion relative to the LEM, expressed in M-Frame coordinates, is:

$$\bar{\rho}_M = \bar{r}_{M/C} - \bar{r}_{M/L}$$

$$\dot{\bar{\rho}}_M = \dot{\bar{r}}_{M/C} - \dot{\bar{r}}_{M/L}$$

3. Rendezvous Radar Interface Parameters.

a. Gimbal Angles. Presented in Figure 8 is a schematic representation of the rendezvous radar gimbaling geometry. Consider a rendezvous radar axes system (x_{RR}, y_{RR}, z_{RR}) fixed to the radar dish. Let the radar axes coincide with the LEM body axes. Define x_{RR}, y_{RR} and z_{RR} directions as the outboard, inboard and boresight axis, respectively. Position the radar axes by a rotation E_{LS} about Y_B, followed by a second rotation A_{LS} about the new X_B' axis so formed. The transformation matrix reduces to:

$$\bar{r}_{RR} = M(E_{LS}, A_{LS})\,\bar{r}_B \qquad \text{(f-3)}$$

or, in expanded form:

$$\begin{bmatrix} x_{RR} \\ y_{RR} \\ z_{RR} \end{bmatrix} = \begin{bmatrix} \cos E_{LS} & 0 & -\sin E_{LS} \\ \sin A_{LS} \sin E_{LS} & \cos A_{LS} & \sin A_{LS} \cos E_{LS} \\ \cos A_{LS} \sin E_{LS} & -\sin A_{LS} & \cos A_{LS} \cos E_{LS} \end{bmatrix} \begin{bmatrix} P_{XB} \\ P_{YB} \\ P_{ZB} \end{bmatrix}$$

Realize that z_{RR} specifies the line-of-sight direction between the vehicles. Hence, component distances x_{RR} and y_{RR} must be zero. Therefore:

$$0 = \rho_{X_B} \cos E_{LS} - \rho_{Z_B} \sin E_{LS} \qquad \text{(f-4)}$$

$$0 = \rho_{X_B} \sin A_{LS} \sin E_{LS} + \rho_{Y_B} \cos A_{LS} + \rho_{Z_B} \sin A_{LS} \cos E_{LS} \qquad \text{(f-5)}$$

Solving equations (f-4) and (f-5) for E_{LS} and A_{LS} gives: $\tan E_{LS} = \dfrac{\rho_{X_B}}{\rho_{Z_B}}$ (F-20)

and

$$\tan A_{LS} = \frac{-\rho_{Y_B}}{\rho_{X_B} \sin E_{LS} + \rho_{Z_B} \cos E_{LS}} \qquad \text{(F-21)}$$

Gimbal angle E_{LS} exhibits a singularity when the CSM line-of-sight lies along the LEM Y_B body axis ($\rho_{X_B} = \rho_{Z_B} = 0$). Geometrically, this condition corresponds to $A_{LS} = \pm \pi/2$ and $E_{LS} = 0$. The indeterminancy, $\tan E_{LS} = 0/0$, is circumvented by introducing logic (F-22) that forces $E_{LS} = 0$ when $\rho_{X_B} = \rho_{Z_B} = 0$.

The line-of-sight gimbal angle rates relative to the body axes are generated by differentiating E_{LS} and A_{LS} with respect to time (see equations F-20, 21). Infinite rates exist when ρ_{Y_B} and ρ_{Z_B} approach zero. Infinite rates are ameliorated by the addition of logic commands (F-22) that force either A_{LS} or E_{LS} to π rad/sec whenever ρ_{Y_B} or ρ_{Z_B} equal zero, respectively.

G. LEM Lunar Landing Radar

1. Purpose. - The purpose of Set G is to determine velocity and altitude inputs for the Landing Radar Math Model and the Lunar Land Mass Simulator. In addition, subsidiary calculations are made to determine the slant range of each landing radar beam measured from the LEM vehicle to the lunar surface. Set G equations are not activated during Earth mission exercises.

2. Doppler Input Velocities

a. The Moon's Shape. - The Moon's surface velocity at the subsatellite point and LEM altitude depend on the Moon's shape. The Land Mass Simulator will be employed to generate surface irregularities above an assumed spherical datum reference (R_{LM}). The datum reference will vary depending on the intended landing site (ϕ_{LM}, λ_{LM}). Since the Land Mass Simulator is designed for 10 specific landing sites, 10 spherical datum references are envisioned (R_{LM_i}; $i = 1, 2 \ldots 10$).

It is common practice to represent the Moon's surface by a triaxial ellipsoid (reference 36)

$$R'_{LM} = a_M(1 - f'(\cos \phi_{LM} \sin \lambda_{LM})^2 - f^* \sin^2 \phi_{LM}) \qquad (g\text{-}1)$$

Parameters f' and f* denote the Moon's equatorial and polar flattening constants, while a_M represents the Moon's semi-major axis. Both the semi-minor equatorial axis and semi-polar axis are foreshortened by approximately 0.2 n.m. and 0.6 n.m., respectively, when compared to a_M. Equations (g-1) may be used to establish the spherical datum reference at problem start. Thus, if the first intended landing site is at the pole, then the Moon's constant radius would be $R_{LM} = a_M (1 - f^*)$.

Altitude errors introduced by the foregoing assumption are small as illustrated by the following example: The landing radar is activated at altitudes below 30,000 feet. Assume the maximum surface range, measured from the subsatellite point to the landing site will always be less than 35 n.m. A 35 n.m. shift in surface location on the reference triaxial ellipsoid causes a maximum selenographic radius error of approximately 5 feet compared to a spherical model. This altitude error is negligible compared to the simulated Land Mass surface irregularities. Consequently all subsequent calculations are referenced to the sperical datum.

b. Velocity of Subsatellite Point. - At any instant, the LEM's subsatellite point in terms of selenographic latitude and longitude is known:

$$\text{Sin } \phi_{S/L} = \frac{Z_{S/L}}{r_{M/V}} ; \quad -\frac{\pi}{2} \leq \phi_{S/L} \leq \frac{\pi}{2}$$

$$\text{Tan } \lambda_{S/L} = \frac{Y_{S/L}}{X_{S/V}} \qquad \text{(G-12)}$$

Where V = L for LEM vehicle

Hence, the vector components of the subsatellite point, measured in selenographic coordinates, can be found:

$$\bar{R}_{S/L} = R_{LM} \left(\text{Cos } \phi_{S/L} \text{ Cos } \lambda_{S/L} \hat{i}_S + \text{Cos } \phi_{S/L} \text{ Sin } \lambda_{S/L} \hat{j}_S + \text{Sin } \phi_{S/L} \hat{k}_S\right) \qquad \text{(G-14)}$$

Accordingly, the lunar surface velocity is given by:

$$\dot{\bar{R}}_{S/L} = \bar{\omega}_S \times \bar{R}_{S/L} \qquad \text{(G-16)}$$

It remains to determine the Moon's total angular velocity $\bar{\omega}_S$.

Note that the Moon's nodal regression rate vector (Figure 6) is parallel to the ecliptic plane. Also, note that the mean position of the Moon is given by the mean longitude, $\mathbb{C}$, which is measured from the mean equinox along the ecliptic to the mean ascending node, and then along the lunar orbit. Since measurements are made with respect to the mean equinox of date, which is assumed fixed, vector $\dot{\mathbb{C}}$ reflects the change of the mean Moon's position relative to the regressing mean ascending node. Consequently, $\dot{\bar{\mathbb{C}}}$ is directed normal to the lunar orbit. From Cassini's Laws, however, the Moon's rate about the north-south axis is equal to the Moon's mean rotation in its orbit. Thus, $\dot{\mathbb{C}}$ is also directed along Z_s. Transforming vectors $\dot{\bar{\Omega}}$ and $\dot{\bar{\mathbb{C}}}$ to selenographic coordinates gives:

$$\begin{pmatrix} W_{Xs} \\ W_{Ys} \\ W_{Zs} \end{pmatrix} = A_{kl} \; A_{lm} \begin{pmatrix} 0 \\ 0 \\ \dot{\Omega} \end{pmatrix} + \begin{pmatrix} 0 \\ 0 \\ \dot{\mathbb{C}} \end{pmatrix} \qquad \text{(g-2)}$$

Matrix operators a_{kl} and a_{lm} are given by subset equations D-13 and D-15.

Equations (g-2) does not include velocities induced by physical librations. These terms are neglected because, even if a conservative libration amplitude of 0.06 deg/year is assumed, then the resulting surface velocity due

to libration is approximately 2×10^{-4} ft/sec. which is insignificant when compared to a surface velocity of about 0.06 ft/sec. for nodal regression and about 13 to 14 ft/sec. for $\dot{\mathfrak{C}}$.

NASA has recommended (reference 40) that the surface velocity due to ($\dot{\Omega}$) be neglected. This is reasonable since the $\dot{\Omega}$ contribution is 20 times smaller than the $\dot{\mathfrak{C}}$ contribution and will have no effect on astronaut training.

Lunar surface velocity components, measured in M-frame coordinates, in general, are now found to be:

$$\dot{\bar{r}}_{M/S} = a_{ij} \dot{\bar{R}}_{S/L} \qquad \text{(G-10)}$$

c. Velocity of LEM Relative to Lunar Surface. - LEM inertial M-frame velocity components are computed from equations A-11. The LEM velocity vector relative to the Moon's surface is, therefore:

$$\dot{\bar{r}}_{M/R} = \dot{\bar{r}}_{M/L} - \dot{\bar{r}}_{M/S} \qquad \text{(G-21)}$$

This relative velocity vector is transformed into body axes using matrix operator g_{ij_M}:

$$\dot{\bar{r}}_{B/S} = g_{ij_M} \dot{\bar{r}}_{M/R} \qquad \text{(G-20)}$$

An additional transformation is required to generate doppler velocity signals measured along landing radar beam directions:

d. Landing Radar Beam Directions. - The Landing Radar Subsystem computes three components of relative velocity and altitude above the lunar terrain. Effectively, these stated parameters are measured by four doppler signals that are transmitted to the surface in a fixed beam pattern relative to the landing radar antenna assembly planar array (Figure 9). Moreover, the landing radar antenna can be positioned in one of two known orientations relative to the LEM X_B - Z_B body axes. These positions ensure that the altitude beam (D_4) will be approximately normal to the lunar surface, as the LEM orientation is altered during the powered descent and hover-to-touchdown mission phases.

Consider the ordered rotations necessary to establish the matrix operator between body axes directions $\hat{X}_B$, $\hat{Y}_B$, $\hat{Z}_B$ and landing radar beam directions $\hat{D}_1$, $\hat{D}_2$, $\hat{D}_3$, and $\hat{D}_4$ (see Figure 9). A single negative rotation ($\alpha_j + \xi_k + \frac{\pi}{2}$; $j = 1, 2$; $k = 1, 2, 3, 4$) about the Y_B body axis defines the altimeter beam

direction i_4, and locates the plane formed by $\hat{i}_1$ and $\hat{i}_2$. A positive (Λ_2) or negative (Λ_1) rotation about the new X'_B axis is sufficient to describe $\hat{i}_2$ or $\hat{i}_1$. A similar procedure is used to locate $\hat{i}_3$. Combining all rotations yield:

$$\begin{bmatrix} D_1 \\ D_2 \\ D_3 \\ D_4 \end{bmatrix} = \gamma_{ij} \begin{bmatrix} X_B \\ Y_B \\ Z_B \end{bmatrix}$$

where (g-1)

$$\gamma_{ij} = \begin{bmatrix} a_1 & b_1 & c_1 \\ a_2 & b_2 & c_2 \\ a_3 & b_3 & c_3 \\ a_4 & 0 & c_4 \end{bmatrix}$$

Fixed matrix elements a, b and c (equations G-47, 48 and 49) are trignometric combinations of the positive-valued, geometric pattern angles ξ_k and Λ_i. Input angles, $\xi_k = \xi_o + \Delta\xi_k$ and $\Lambda_i = \Lambda_o + \Delta\Lambda_i$, reflect the nominal design angles of each radar beam relative to the landing plate, plus calibration errors.

Finally, doppler velocity input signals to the Landing Radar Math Model are found from equations (g-3) and (G-20):

$$\begin{bmatrix} D_{S_1} \\ D_{S_2} \\ D_{S_3} \end{bmatrix} = q_{ij} \begin{bmatrix} \dot{X}_{B/S} \\ \dot{Y}_{B/S} \\ \dot{Z}_{B/S} \end{bmatrix} \qquad \text{(G-40)}$$

Doppler signals D_{s_1}, D_{s_2}, D_{s_3} do not include spurious velocity signals, transmitted to the landing radar angenna assembly, due to vehicle CG rotation rates p_b, q_b, r_b. These velocities are small, have an average value of zero and are therefore neglected.

It remains to determine the actual altitude above the lunar terrain as well as the slant range of each radar beam.

3. Slant Range Measured Along Radar Beams

a. General. Slant range calculations depend on two geometric angles. These are:

i. The angle μ_k measured between each doppler beam direction and the LEM local vertical (Figure 10).

ii. The angle θ_{O_k} measured between each doppler beam direction and the local vertical formed by the intersection of each doppler beam with the lunar surface (Figure 10).

b. Local Vertical Angle. Angle μ_k is formed by taking the dot product of each beam direction (g-3) with the LEM radius vector defined with respect to the landing radar plate rather than the vehicle CG:

$$\cos \mu_k = \frac{\bar{r}'_{B/L} \cdot \hat{\imath}_k}{\left|\bar{r}'_{B/L}\right|} \qquad (G\text{-}43)$$

$$0 \leq \mu_k \leq \frac{\pi}{2}$$

where, the radius vector from the moon to the landing radar antenna origin is:

$$\bar{r}'_{B/L} = \bar{r}_{B/L} + \bar{\alpha}_{LR}\,\hat{i}_B + \bar{\beta}_{LR}\,\hat{j}_B + \bar{\gamma}_{LR}\,\hat{k}_B \qquad (G\text{-}41)$$

and where:

$$\bar{r}_{B/L} = g_{ij_M}\,\bar{r}_{M/L} \qquad (G\text{-}42)$$

Vectors $\bar{r}_{B/L}$ and $\bar{r}'_{B/L}$ are illustrated below:

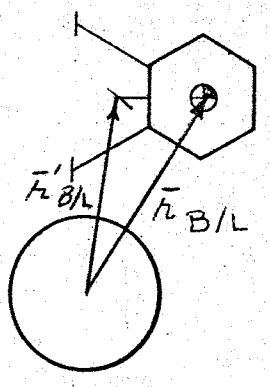

Should μ_k be greater than $\frac{\pi}{2}$, then an intersection between the k^{th} radar beam and the lunar surface is impossible. In fact, the limiting condition is specified by the angle measured between the LEM local vertical at the landing radar antenna assembly and a line drawn from the LEM tangent to the lunar surface. Call this angle μ_{max}, hence:

$$\sin \mu_{max} = \frac{R_{IM}}{r'_{B/L}} \qquad (G\text{-}43b)$$

$$0 \leq \mu_{max} \leq \frac{\pi}{2}$$

If $\mu_k > \mu_{max}$, then the k^{th} beam will not intersect the lunar surface; consequently, $R_k = \infty$(G-43a). Logic given by (G-43a) must be programmed to prevent a singularity from occurring in loops G-44 and G-45.

c. Surface Intersection Angle and Slant Range. - Angle θ_{o_k} is computed from the law of sines whenever $\mu_K \leq \mu_{MAX}$:

$$\sin \theta_{o_k} = \frac{r'_{B/L}}{R_{LM}} \sin \mu_k \qquad (G\text{-}44)$$

$$0 \leq \theta_{o_k} \leq \frac{\pi}{2}$$

Angle θ_{o_k} is a Landing Radar Math Model input that characterizes the backscattering effect as each doppler beam makes contact with the lunar surface.

The slant range, measured from the radar plate origin along each doppler beam to its intersection with the assumed datum surface is:

$$R_k = R_{LM} \frac{\sin (\theta_{o_k} - \mu_k)}{\sin \mu_k} \qquad (G\text{-}45)$$

d. Altitude Above Reference Datum. - Two idealized altitude signals relative to the spherical datum surface are computed for use on the instructor's console. Altitudes $h_{M/L}$ and $h_{M/LR}$ are measured from the datum surface to the vehicle CG and landing radar antenna assembly, respectively:

$$h_{M/L} = r_{M/L} - R_M \qquad (G\text{-}30)$$

$$h_{M/LR} = r'_{B/L} - R_M$$

The differences in altitude ($h_{M/L} - h_{M/LR}$) may be as large as 8 feet. Altitude rate is given by:

$$\dot{h}_{M/L} = \frac{\bar{r}_{M/L} \cdot V_{M/L}}{|\bar{r}_{M/L}|} = \dot{r}_{M/L} \qquad (G-30)$$

Local surface irregularities are not reflected by equations (G-30, 45). Terrain elevation above the reference datum will be specified by the Landmass Simulator to modify the ideal altimeter range signal R_4. Corrections will not be made to slant range measured along doppler velocity beams R_1, R_2 and R_3.

4. Landmass Simulator.

a. General. - A Landmass Simulator, consisting of a film plate transport and an optical-electrical system, provides local elevation information for 10 specific areas of the moon. The film transport represents a planar surface tangent to the moon at one of the ten intended landing sites.

The landmass film will be referenced to the External Visual Display Equipment MEP film coordinates, identically to the Landing and Ascent visual system (see paragraph J-4). Therefore, the landmass coordinates are:

$$Y_{LM} = Y_{LA}$$
$$Z_{LM} \neq Z_{LA} \qquad (G-50)$$

Surface irregularities above the reference datum are projected onto the flat film transport (see sketch) and subsequently read by an optical-electrical system. In essence, the optical-electrical system is positioned

relative to the LEM subsatellite point, whereupon an additional signal (ψ_{LM}) is generated to locate the vector drawn from the subsatellite point to the altimeter beam intersection point (Figure 11).

The beam intersection with the lunar surface is known in selenographic coordinates $(X,Y,Z)_{S/4}$ (G-62). This point is then transformed into film coordinates $\delta_{S/4}$, $\Theta_{S/4}$ (G-63), and compared to the landmass film reference points δ_{LM}, Θ_{LM}.

Thus:

$$\Delta Y_4 = K_o \ (\Theta_{S/4} - \Theta_{LM})$$
$$\Delta Z_4 = K_o \ (\delta_{S/4} - \delta_{LM}) \qquad \text{G-64}$$

where: $K_o = 0.9952557 \times 10^6$ ft/deg and is the small angle approximation to correct ΔY_4 and ΔZ_4 into feet.

Therefore: the beam azimuth can be derived:

$$\psi_{LM} = \tan^{-1} \frac{\Delta Y_4 - Y_{LM}}{Z_4 - Z_{LM}} \qquad \text{G-60}$$

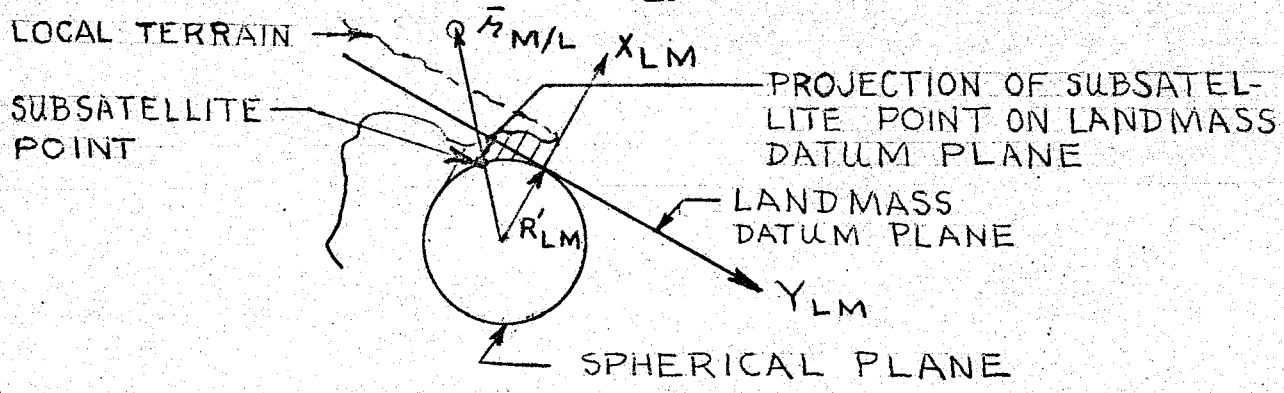

Given ψ_{LM}, Y_{LM}, Z_{LM} and μ_4, the Landmass Simulator automatically outputs surface elevation, e_t (Figure 10), normal to the film transport. This signal is resolved along the alitmeter beam and mixed with R_4 to yield an indicated altitude R'_4:

$$R'_4 = R_4 - \frac{e_t}{\cos \Theta_{o_4}} \qquad \text{(G-46)}$$

11/65

H. LEM-Earth, LEM-CSM Communication Requirements

1. Purpose.- The purpose of Set H is to determine whether or not the LEM can communicate with either the CSM or Earth tracking stations. The LEM-VHF antennas are used to communicate with the CSM. An S-band antenna or two fixed, conical log antennas are used for Earth communications, while in lunar orbit or Earth orbit, respectively.

2. LEM-CSM Communication Capability

a. Line-of-Sight Viewing.- LEM-CSM visibility constraints are based on the orientation of the line-of-sight vector $\bar{\rho}^*$ relative to the central body. During lunar or terrestrial operations the Moon or Earth, respectively, is regarded as the central body. Geometric visibility constraints are generalized and apply to either mission model

As shown in Figure 12a, visibility is assured if R_c^* is greater than the central body radius. Distance R_c^* is computed below:

But: $$R_c^* = r_{n/c} \operatorname{Sin} B_c \qquad \text{(h-1)}$$

$$\operatorname{Sin} B_c = \frac{r_{n/L} \operatorname{Sin} \sigma_c}{\rho_{LS}} \qquad \text{(h-2)}$$

Substituting (h-2) into (h-1) gives:

$$R_c^* = \frac{r_{n/c}\, r_{n/L} \operatorname{Sin} \sigma_c}{\rho_{LS}} \qquad \text{(H-11)}$$

Angle σ_c is defined by the scalar product of $\bar{r}_{n/c}$ and $\bar{r}_{n/L}$, or:

$$\operatorname{Cos} \sigma_c = \frac{\bar{r}_{n/L} \cdot \bar{r}_{n/c}}{\left|\bar{r}_{n/L}\right| \left|\bar{r}_{n/c}\right|} \qquad \text{(H-12)}$$

$$0 \leq \sigma_c \leq \pi$$

Visibility may also be possible when R_c^* is less than R_n (Figure 12a). This condition is tested based on a comparison between angles σ_c and σ_c^*, defined in Figure 12a. Note that:

$$\operatorname{Cos} \sigma_c^* = \frac{R_n}{r_{n/c}} \qquad \text{(H-11)}$$

$$0 = \leq \sigma_c^* \leq \frac{\pi}{2}$$

Equations H-11 and H-12 are interpreted as follows:

i. Visibility always exists if $R_c^* < R_n$ provided $\sigma_c \leq \sigma_c^*$.

ii. Visibility never exists if $R_c^* < R_n$ and $\sigma_c > \sigma_c^*$.

iii. Visibility always exists whenever $R_c^* \geq R_n$.

b. VHF Antenna Orientations. - Even though the CSM and LEM are visible to one another, the CSM and LEM-VHF antennas may be misaligned such that a high noise to signal strength ratio precludes communication. A requirement is established, therefore, to define VHF antenna orientations. These orientations are specified by the angle:

i. ξ_{Li}, measured between the LEM antenna and the line-of-sight.

ii. ξ_{ci}, measured between the CSM antenna and the line-of-sight.

iii. ζ_{ii}, measured between the LEM and CSM antennas projected on a plane perpendicular to the line-of-sight.

Angles ξ_{Li}, ξ_{ci} and ζ_{ii} are required inputs to the Communication Math Model.

Each vehicle has two VHF antennas. At any instant, only one antenna on either vehicle, selected by the astronauts, will be used for communication. The choice of antennas must be inputted to the LMS Math Model.

Consider angle ξ_{Li} calculations. The direction cosines of each LEM antenna relative to the LEM body axes is known:

Via the general equations $\hat{W}_{ji} = \hat{W}_{1i}\,\hat{\imath}_B + W_{2i}\,\hat{j}_B + W_{3i}\,\hat{k}_B$

Derive:

$$\hat{l}_i = l_{ij}\hat{\imath}_B + l_{2i}\,\hat{j}_B + \hat{l}_{3i}\,\hat{k}_B \qquad \text{(H-51)}$$

$$i = 1, 2$$

Similarly, the direction cosines of each CSM antenna relative to the CSM body axis is known:

$$\hat{C}_i = C_{ij}\,\hat{\imath}_{B_c} + C_{2i}\,\hat{j}_{B_c} + C_{3i}\,k_{B_c} \qquad \text{(H-51)}$$

$$i = 1, 2$$

Vectors $\hat{L}_i$ and C_i are further resolved to M or E frame coordinates:

$$\hat{l}_{ni} = g^T_{ijn}\,\hat{l}_j \qquad \text{(H-52)}$$

$$\hat{C}_{ni} = g^T_{ijc}\,\hat{C}_k \qquad \text{(H-53)}$$

During independent operation, the CSM antenna direction cosines (H-51) are required IMS inputs. The IMS will compute the CSM, n-frame vector $\hat{C}_{ni}$ (H-53). During integrated operations, however, the AMS will compute all CSM-VHF antenna directions.

The desired angles measured between the line-of-sight direction, $\bar{\rho}^*$, and each antenna direction (see sketch) can be found:

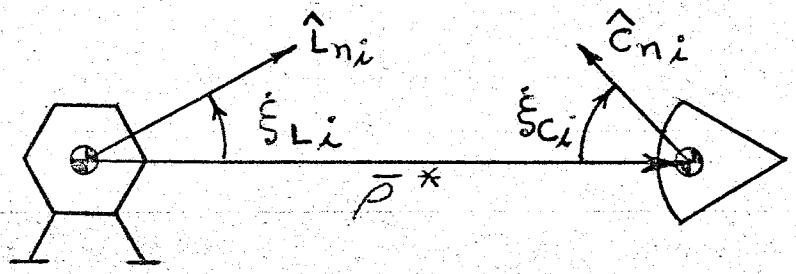

$$\cos \xi_{Li} = \frac{\bar{\rho}^* \cdot L_{ni}}{|\bar{\rho}^*|} \qquad 0 \le \xi_{Li} \le \pi$$

$$\cos \xi_{ci} = -\frac{\bar{\rho}^* \hat{C}_{nj}}{|\bar{\rho}^*|} \qquad 0 \le \xi_{ci} \le \pi \qquad \text{(H-50)}$$

In order to define angle ζ_{ii}, the directions normal to the planes formed by the LEM antennas and $\bar{\rho}^*$, and the CSM antennas and $\bar{\rho}^*$ must first be ascertained These directions are:

$$\hat{n}_{Li} = \frac{\bar{\rho}^* \times \hat{L}_{ni}}{|\bar{\rho}^*| \sin \xi_{Li}}$$

$$\hat{n}_{ci} = \frac{\bar{\rho}^* \times \hat{C}_{ni}}{|\bar{\rho}^*| \sin \xi_{ci}} \qquad \text{(h-54)}$$

Now, ζ_{ii} is:

$$\cos \zeta_{ii} = \hat{n}_{Li} \cdot \hat{n}_{ci}$$

$$0 \le \zeta_{ii} \le \pi \qquad \text{(H-54)}$$

c. S-Band Antenna Orientation - Lunar Phase Missions. - Whenever the visibility requirements are satisfied, a final test must be made to determine whether or not the LEM can communicate with the Earth. This test demands that the S-band antenna be pointed in a desired direction and remain within allowable gimbal limits.

Ideally, the antenna should be pointed toward the Earth's center (lunar mission). This direction is:

$$\bar{r}_M = -(\bar{r}_{M/L} + \bar{r}_{E/M}) \qquad \text{(H-43)}$$

Resolving equations H-43 into body coordinates gives the direction required for S-band pointing:

$$\bar{r}_{BM} = g_{ij_M}\, \bar{r}_M \qquad \text{(H-45)}$$

Figure 13 presents the S-band gimbal geometry. This geometry corresponds to the rendezvous radar gimbal geometry (Figure 8) discussed earlier. Thus, rendezvous radar equations f-3, f-4 and f-5 define the relationships between S-band coordinates and body coordinates provided E_{LS} and A_{LS} are replaced by Θ_c and ϕ_c, respectively. The desired S-band gimbal angles, for communication, are therefore:

$$\text{Tan}\ \Theta_c = \frac{X_{BM}}{Z_{BM}} \qquad \text{(H-40)}$$

$$\text{Tan}\ \phi_c = \frac{-Y_{BM}}{X_{BM}\ \text{Sin}\ \Theta_c + Z_{BM}\ \text{Cos}\ \Theta_c} \qquad \text{(H-42)}$$

Angles Θ_c and ϕ_c are inputted to the Communication Math Model and compared to the allowable S-band gimbal angles. If Θ_c and ϕ_c lie within allowable limits, then communication is possible; otherwise, the LEM orientation must be altered before communication can commence.

d. Conical Lag Antenna Orientation. - Two conical lag spiral-fixed antennas are used as an emergency backup for the S-band steerable antenna when in lunar orbit and for Earth communication when in Earth orbit. The signal to noise ratio is dependent on the angle ξ'_i measured between the

antenna direction $\hat{l}'_c$ and the line-of-sight direction (see sketch).

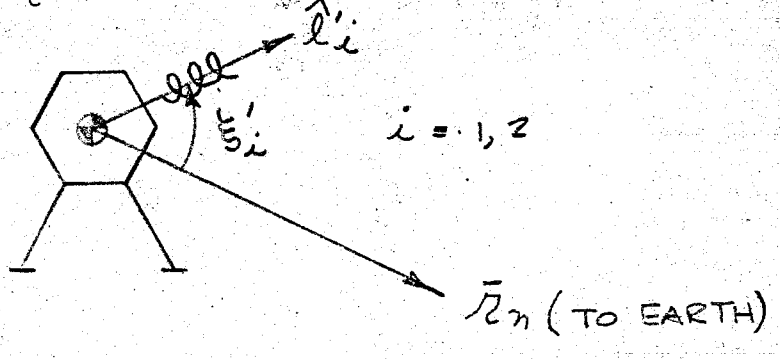

The body fixed antenna directions are known via the general equation

$$\hat{W}_{ji} = W_{ij}\,\hat{i}_B + W_{2i}\,\hat{j}_B + W_{3i}\,\hat{k}_B$$

$$\hat{l}_i' = l'_i\,\hat{i}_B + l_2'\,\hat{j}_B + l_3'\,\hat{k}_B \qquad \text{(H-51)}$$

$$i = 1, 2$$

Resolving these coordinates into M or E frame coordinates gives:

$$\hat{l}_{n_i}' = g_{ij_n}^{T}\,\hat{l}'_i \qquad \text{(H-52)}$$

I. Weights and Balance.

1. Purpose. - The purpose of Set I is to compute the instantaneous LEM mass, center of gravity, and moments and products of inertia. Subsidiary calculations are made to define reference distances measured from the vehicle CG to specific subsystem centroids.

2. LEM Mass. - An attempt is made to simplify the mass breakdown of the LEM vehicle. Mass calculations, equation I-10, are characterized by constant and variable mass groups. Component mass contributions to each group follow.

a. Constant Masses. - The total dry mass of the ascent (m_I) and descent (m_{II}) stages are invariant initial inputs. These constants masses do not include propellant mass but do include expendables ejected during the ascent or descent phases. During an actual mission, mass is continually expended in the form of vented material, gas leaks, waste management, etc. It is assumed that all expendables are included as a rigid part of the ascent (m_I), or descent (m_{II}) stages.

In the event that the CSM propulsion system malfunctions, the LEM propulsion system will be required to initiate the trans-earth maneuver. Since the LEM and CSM must be attached during this emergency condition, the total system mass must reflect the CSM mass, m_c. Mass m_c represents a constant input whenever the vehicles are attached during independent IMS mission modes. Mass m_c, together with component distances α_c, β_c and γ_c, measured from the CSM-CG to the weights and balance reference axes will be supplied by the AMS during integrated operations.

b. Variable Masses. - Variable masses include all propellants only. Main engine ascent (m_{Aj}) and descent (m_{Dj}) fuel and oxidizer masses are supplied by the propulsion Math Model (I-12). RCS system a and b propellants are computed by the RCS Math Model and inserted as inputs to interface equations (I-11).

3. Instantaneous Center-of-Gravity. - The LEM-CG is found by summing the product of all component masses and their local reference arms measured from the 0, 0, 0 origin of the design reference system (I-20). Note that most reference arms are constant inputs that remain invarient during any run. These include the arms corresponding to the dry masses (v_I, v_{II};

$v \rightarrow \alpha, \beta, \gamma$), the RCS propellants ($v_{Rj}$), the ascent propellants (v_{Aj}) and the β_{Dj} and γ_{Dj} components of the descent propellants. Component distances α_{Dj} are computed variables that reflect the combined mass centers of the rigid propellant CG's and the slosh propellant CG's. The slosh propellant CG is defined by the slosh model pendulum support hinge.

Slosh forces are zero whenever the main engine is inoperative. For this condition, the propellant moves to the bank periphery and the moment arm α_{Dj} goes to zero (equation A-48 and Figure 4).

4. Moments and Products of Inertia. - Moments and products of inertia may be computed by a direct or indirect method. Direct computations require that each component mass first be located relative to the total vehicle CG ($\bar{v} = v + v_{CG}$) and then transferred to the instantaneous LEM-CG. Component reference distances, $\bar{v}$, are time dependent, since the vehicle CG varies as mass is expended. Thus, the squares and products of each reference distance must be continually computed. These calculations impose large storage requirements on the computer.

Indirect calculations are based on defining moments and products of inertia with respect to the invariant design reference origin and subsequently transferring these inertias to the instantaneous CG. Indirect rather than direct calculations are preferred since reference distances, v, required to specify the inertias with respect to the reference origin (I-41, 51), are constant inputs except for v_{Dj}. Even when the transfer terms are included (I-40, 50), the computations required to program the indirect method are less than those required to program the direct method.

Ascent and descent propellants are treated as mass points in all inertia computations. The reason for this assumption follows (reference 36).

Fuel-oxidizer slosh forces are considered as a perturbation to the rigid body equations of motion. In the absence of viscosity, these first order fluid pressure forces are directed radially outward from each tank. Hence, there can be no moment induced by the fluid about the effective tank centroid. With regard to the spherical ascent tank, the effective centroid coincides with the geometric center. Small motions exist between the effective, cylindrical descent tank centroid and geometric centroid (references 6 and 7). On these bases, effective propellant inertias are computed by assuming that all the propellant mass is concentrated at the effective tank centroid which represents the support hinge of the mechanical pendulum

analog (see Section III-A-4). Experimental data (reference 36) have indicated that, "This approach of calculating rigid body inertias should give substantially more realistic results than would be obtained by assuming the propellant in each tank frozen and concentrating this frozen mass at its center of gravity".

J. Visual Dispaly Drive Equations.

1. Purpose. - The purpose of Set J is to generate drive signals for the External Visual Display Equipment (EVDE). This equipment provides real world visual cues to the astronauts during all lunar and Earth mission modes. Realistic motion may be perceived through each of three windows or three telescope positions.

Optical simulations are generated by four primary hardware subsystems. Briefly, the star field is generated by a Celestial Sphere subsystem. Stars can be occulted by the Moon, Earth or Sun. A Mission Effects Projector (MEP) enables the astronauts to view the lunar or Earth terrain during orbital operations. Detailed landing site viewing is provided by the Landing and Ascent Image Generator. CSM visual sightings are generated by a Rendezvous and Docking Image Generator.

No attempt is made to define the mechanical-optical details of each hardware item since these details are available in numerous Farrand documents. An EVDE hardware summary report is given in reference 37. Equivalent drive signals required to activate each hardware item are derived below.

2. Celestial Sphere.

a. Gimbal Drives. - Four Celestial Spheres, one for each window and one for all telescopes, are used to present an infinity star display to the astronauts. Each Celestial Sphere contains 997 stars referenced to the mean ecliptic of 1950, of which 54 stars are used for navigation. Star motion is simulated by positioning the Celestial Sphere relative to the astronauts, or more appropriately, relative to the body-fixed optical axes (Figure 7).

Presented in Figure 14a is a schematic of the Celestial Sphere gimbal assembly. Motion about the outer (a_{pq})* and middle (b_{pq}) gimbal axes are shown. Inner gimbal motion is mechanized by rotating the Northern and Southern hemispheres relative to a split ring which represents the ecliptic

* As mentioned earlier, generalized subscript p refers to window (W) or telescope (T) viewing, while q denotes the viewing mode, either left (l) or right (r) or above (a).

plane. Arbitrary orientations of the star field can, therefore, be achieved by independent gimbal angle inputs a_{pq}, b_{pq} and c_{pq}. For example, let the Celestial Sphere gimbal axes be initially aligned to the window axes Z_{pq}, Y_{pq}, X_{pq}. Rotate through angle a_{pq} about the optical line-of-sight axis Z_{pq}. Follow this by a rotation b_{pq} about the new Y'_{pq} axis so formed. Finally, follow this by a rotation c_{pq} about the north ecliptic pole to generate the general transformation between the Celestial Sphere axes and the optical axes (Figure 14b):

$$\begin{bmatrix} x_{\mathbb{E}_{pq}} \\ y_{\mathbb{E}_{pq}} \\ z_{\mathbb{E}_{pq}} \end{bmatrix} = \begin{bmatrix} \text{Cos } C_{pq} \text{ Sin } C_{pq} & \text{Sin } a_{pq} \text{ Sin}_{pq} & \text{Cos } b_{pq} \text{ Cos } c_{pq} \\ +\text{Sin } a_{pq} \text{ Sin } b_{pq} \text{ Cos } c_{pq} & -\text{Cos } a_{pq} \text{ Sin } b_{pq} \text{ Cos } c_{pq} & \\ +\text{Cos } a_{pq} \text{ Cos } c_{pq} & +\text{Sin } a_{pq} \text{ Cos } c_{pq} & -\text{Cos } b_{pq} \text{ Sin } c_{pq} \\ -\text{Sin } a_{pq} \text{ Sin } b_{pq} \text{ Sin } c_{pq} & +\text{Cos } a_{pq} \text{ Sin } b_{pq} \text{ Sin } c_{pq} & \\ -\text{Sin } a_{pq} \text{ Cos } b_{pq} & -\text{Cos } a_{pq} \text{ Cos } b_{pq} & \text{Sin } b_{pq} \end{bmatrix} \begin{bmatrix} X_{pq} \\ Y_{pq} \\ Z_{pq} \end{bmatrix} \qquad (j\text{-}1)$$

or:

$$\bar{r}_{\mathbb{E}_{pq}} = A_{ij_{pq}} \bar{r}_{pq}$$

Effectively, equations (j-1) represent the mechanical transformation between optical and ecliptic axes. This transformation can also be generated from computed trajectory data. Recall that equations (D-80) relate the optical axes to the M or E-frame. A single rotation about the equinox $\hat{X}_n$, through the obliquity of the ecliptic, ϵ, is sufficient to reference the optical axes to the ecliptic axes. Thus:

$$\bar{r}_{\epsilon_{pq}} = n_{ij_{pq}} \bar{r}_{pq} \qquad (j\text{-}2)$$

where:

$$n_{ij_{pq}} = \begin{pmatrix} 1 & 0 & 0 \\ 0 & \text{Cos } \mathbb{E} & \text{Sin } \mathbb{E} \\ 0 & -\text{Sin } \mathbb{E} & -\text{Cos } \mathbb{E} \end{pmatrix} l_{ij_{pq}} \qquad (J\text{-}12)$$

1191

8/65

But, equation (j-2) is identical to equation (j-1). Hence:

$$A_{ij_{pq}} = n_{ij_{pq}} \qquad \text{(j-3)}$$

Solving for the unknown gimbal angle drive inputs a_{pq}, b_{pq}, and c_{pq} in terms of known elements $n_{ij_{pq}}$ gives the required drive inputs shown by equation (J-10).

Equation (j-10) exhibits a singularity when the middle gimbal angle b_{pq} approaches $\pm \frac{\pi}{2}$. This condition is circumvented by the introduction of gimbal lock logic (J-11). Logic (J-11) was derived based on the considerations given in paragraph III-D-4e.

b. Lunar or Earth Occulters. Mechanical provisions are included to obstruct the star field whenever the Moon or Earth appears in the windows or telescopes during lunar or Earth Mission modes, respectively. In order to occult the stars, it is required to locate the Moon or Earth relative to the optical axes. This is readily accomplished since the position vector of the central body ($\bar{r}_{B/L}$, G-42) in LEM body coordinates is known. Thus:

$$\bar{r}^{n}_{pq} = - h_{ij_{pq}} \bar{r}_{B/L} \qquad \text{(J-20)}$$

Superscript n denotes either the Moon (M) or Earth (E). The negative sign is needed to direct the vector from the body axes origin to the M or E-frame origin.

A disc of varying diameter is used to occult the star field. As shown is Figure 15, the disc moves in a plane relative to the line-of-sight optical axis and has coordinates given by:

$$\rho'_{pq} = \text{TAN}^{-1} \frac{\left[\left(X^{n}_{pq} \right)^2 + \left(Y^{n}_{pq} \right)^2 \right]^{\frac{1}{2}}}{Z^{n}_{pq}}$$

$$\text{Tan } \theta^{n}_{pq} = \frac{Y^{n}_{pq}}{X^{n}_{pq}} \qquad \text{(J-23)}$$

The field of view measured in the plane of the disc can be approximated by a circle of maximum radius $\rho_{pq_{max}}$. Whenever ρ_{pq} is greater than this distance, the central body cannot be seen. To ensure, however, that the

central body re-enters the window at the correct position, the angle θ_{pq} is continually computed. The ρ_{pq} drive in the EVDE requires only positive valued angles between 0° and 150°. The following logic performs this task as well as the control for operations outside the field of view.

Let $B_1 = 1$ when $210^\circ > \rho_{pq} > 150^\circ$ (J-24)

$B_2 = 1$ when $\rho_{pq} \geq 210^\circ$

Then

$$\rho_{pq} = (\rho_{pq} \bar{B}_1 + \rho_{max} B_1)(\bar{B}_2 - B_2) + (360^\circ) B_2 \quad \text{(J-23)}$$

where $\rho_{max} = 150^\circ$

The occulting discs for the upper window and telescope viewing modes are driven by a mechanical device that requires cartesian rather than polar coordinate inputs, thus:

$$x_{pq} = \rho_{pq} \cos \theta_{pq}$$
$$y_{pq} = \rho_{pq} \sin \theta_{pq} \quad \text{(J-22)}$$

Occulting logic described above also pertains to equation (J-22).

As the vehicle approaches the central body, the body's apparent diameter increases. This effect is simulated by representing the disc as a variable wrap-up reel containing mylar tape. The disc diameter and rate of wrap-up is proportional to the central angle μ^* (μ_{max}, Figure 10) subtended by the LEM. Hence:

$$\sin \mu^* = \frac{R_n}{r_{n/L}} \quad ; \quad 0 \leq \mu^*$$
$$\dot{\mu}^* = -\frac{\dot{r}_{n/L}}{r_{n/L}} \tan \mu^* \quad \text{(J-21)}$$

A configuration can exist when the LEM is behind the Earth or Moon, wherein both central bodies occult the star field. During lunar mission operations, Earth occultation will be synthesized by physically pasting a configuration of the Earth on the Celestial Sphere. The Earth's position in the star field will be based on the Earth's right ascension and declination